OPTICAL SPECTROSCOPY OF THE TRANSITIONAL MILLISECOND PULSARS PSR J1023+0038

UNIVERSITÀ DEGLI STUDI DI MILANO

INAF ISTITUTO NAZIONALE DI ASTROFISICA

The many tones of accretion

To the memory of Tomaso Belloni

07/09/2026 - 11/09/2026

Marco Maria Messa

M. C. Baglio & P. D'Avanzo

INAF, Astronomical observatory of Brera - Merate (LC)

Università Statale di Milano - Milano (MI)

TMSP IN GENERAL

Radio pulsar state

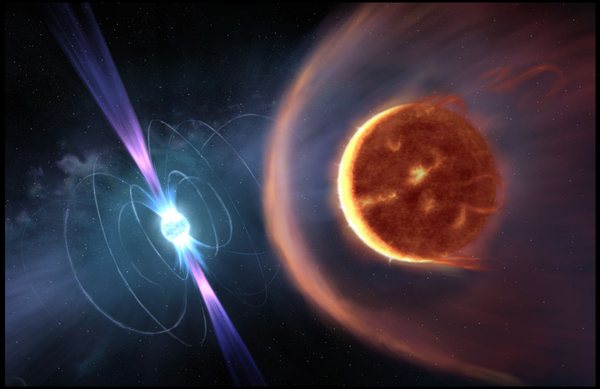

t ~ days/weeks

X-ray pulsar disk state

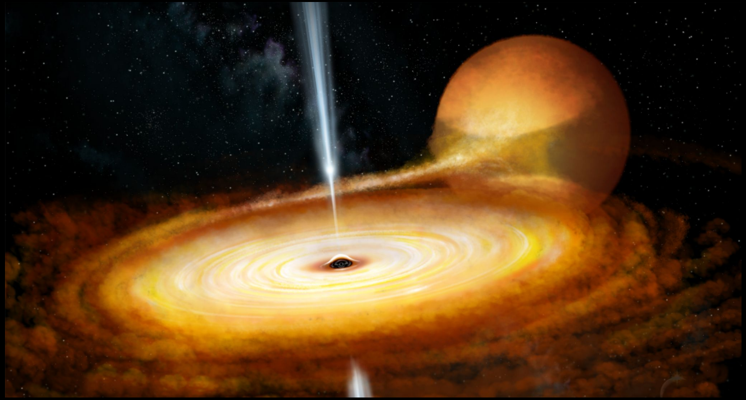

Credit: John Paice

SUB-LUMINOUS DISC STATE

SUB-LUMINOUS DISC STATE

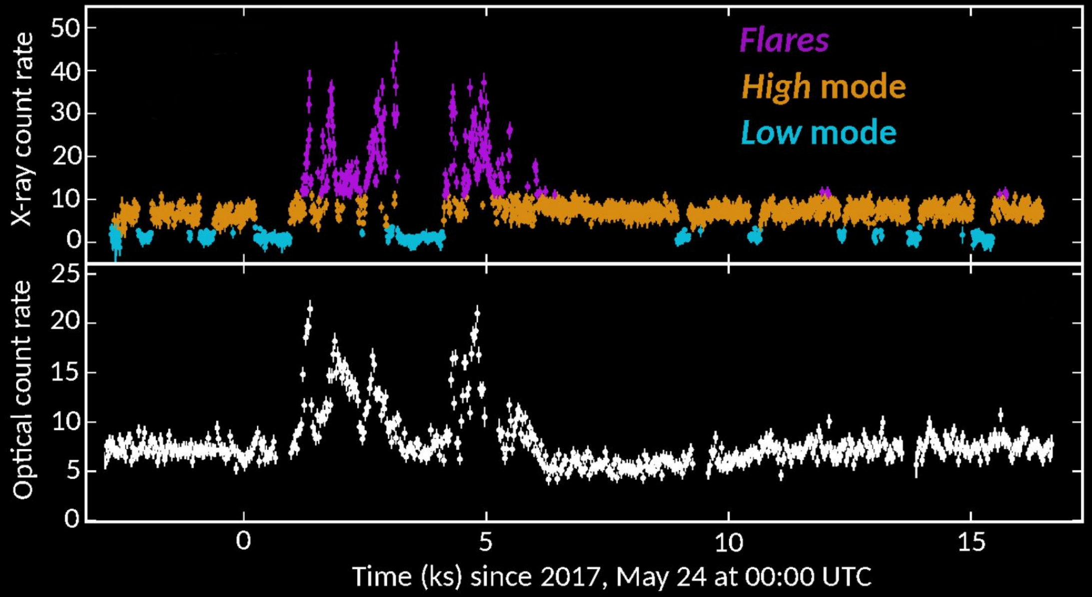

A. Papitto & de Martino, 2022

SUB-LUMINOUS DISC STATE

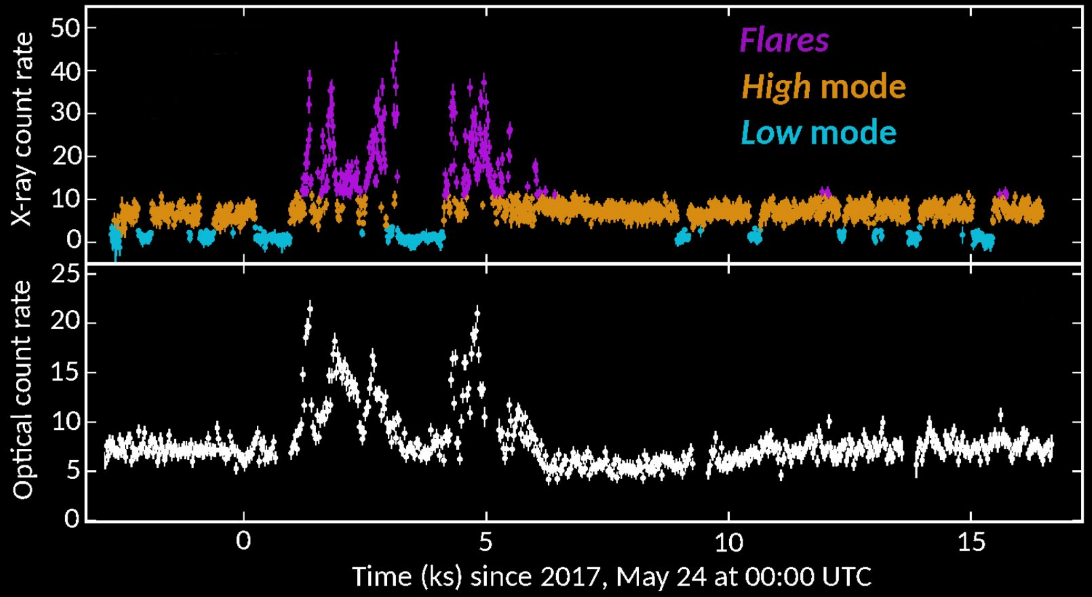

A. Papitto & de Martino, 2022

CXOU J110926.4−650224

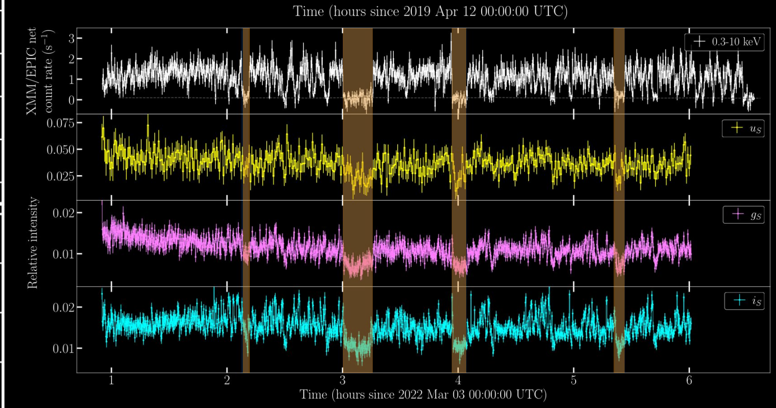

Coti Zelati+, 2024

SUB-LUMINOUS DISC STATE

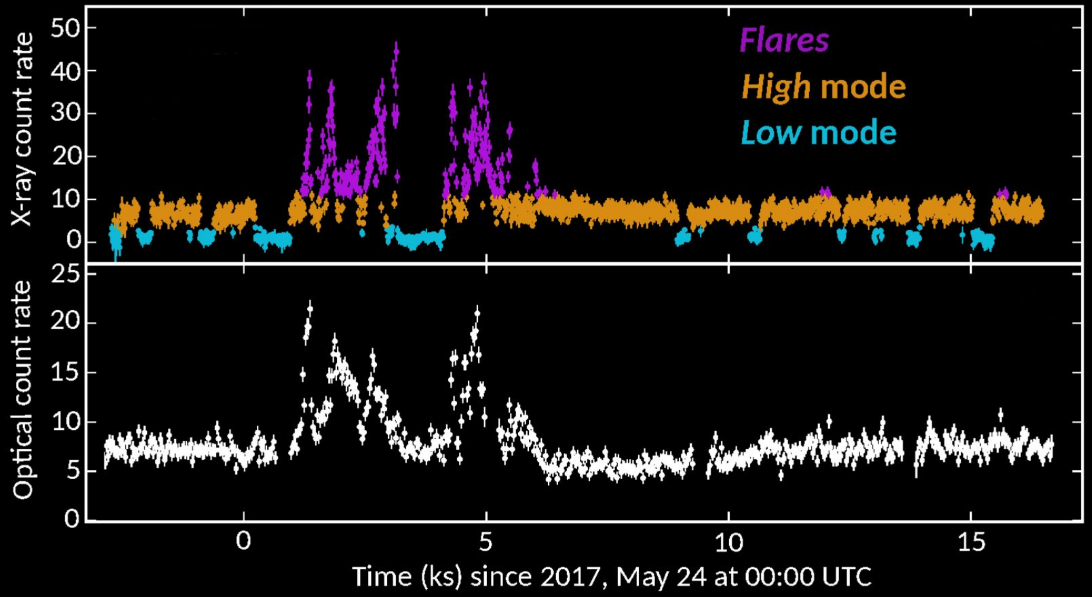

A. Papitto & de Martino, 2022

Papitto et al., 2013
Linares, 2014
Bogdanov et al., 2015
Archibald et al., 2015
Ambrosino et al., 2017
Papitto et al., 2019
Veledina et al., 2019
Campana et al., 2021
Miraval Zanon et al., 2022
Illiano et al., 2023
Baglio & Coti Zelati et al., 2023

and many others!!!!!!!!!!

switches of flux intensity

switches of flux intensity
changes in the accretion flow

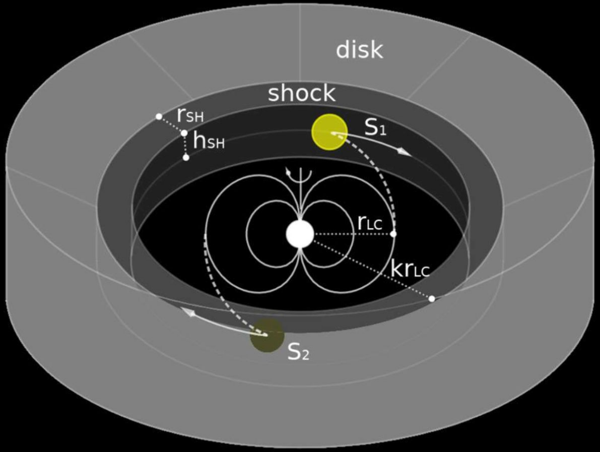

Papitto+, 2019

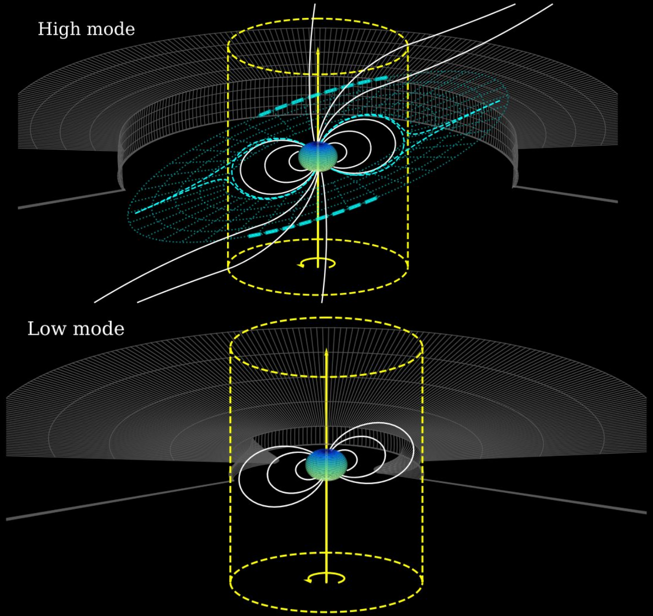

Veledina+, 2019

switches of flux intensity
changes in the accretion flow
geometry of the disc

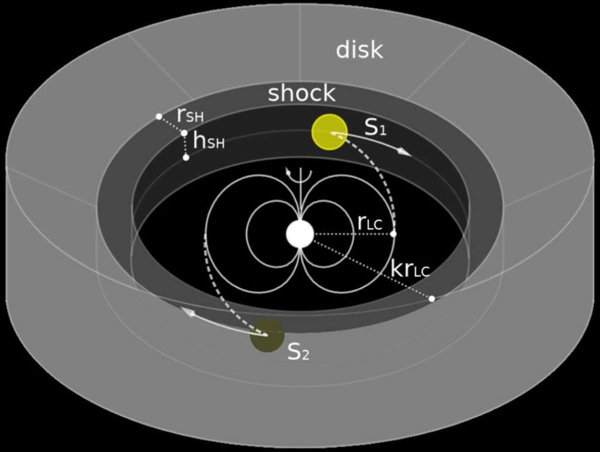

Papitto+, 2019

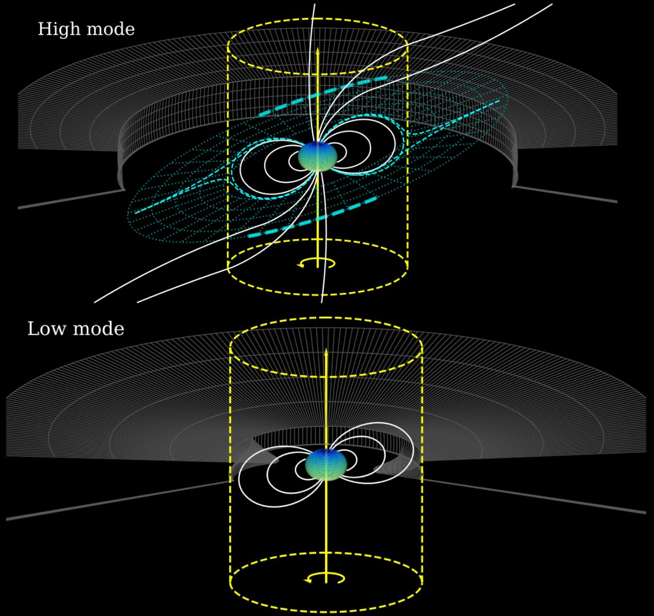

Veledina+, 2019

switches of flux intensity
changes in the accretion flow
geometry of the disc
emission line properties

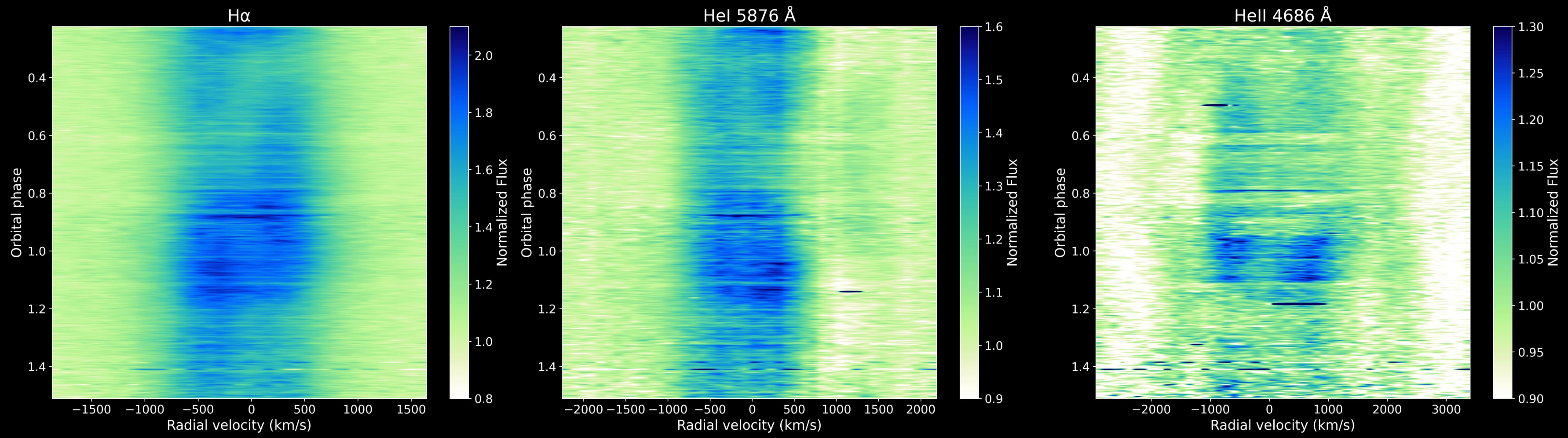

Messa+, accepted to A&A

switches of flux intensity

changes in the accretion flow

geometry of the disc

emission line properties

OPTICAL SPECTROSCOPY AT THE SAME TIMESCALES

OPTICAL SPECTROSCOPY WITH HIGH TEMPORAL RESOLUTION

PSR J1023+0038

Gran Telescopio CANARIAS (GTC)
(PI Coti Zelati)

March 2024

Grism R1000B, R ~1000

One spectrum every ~ 50 sec

Total of 480 spectra

AVERAGE SPECTRUM

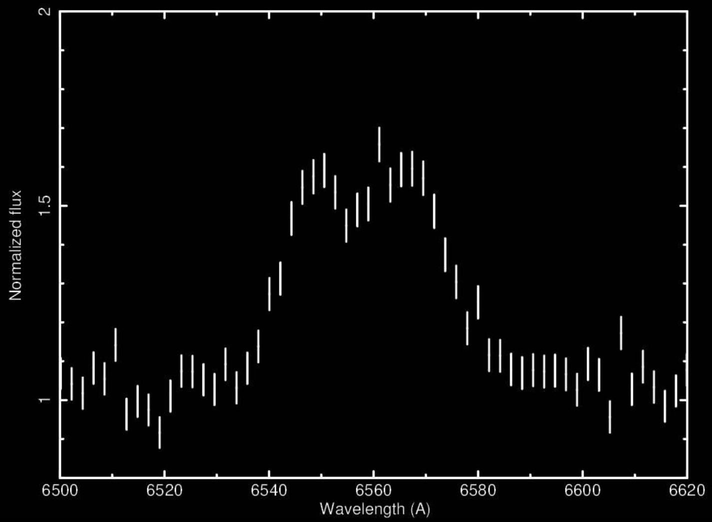

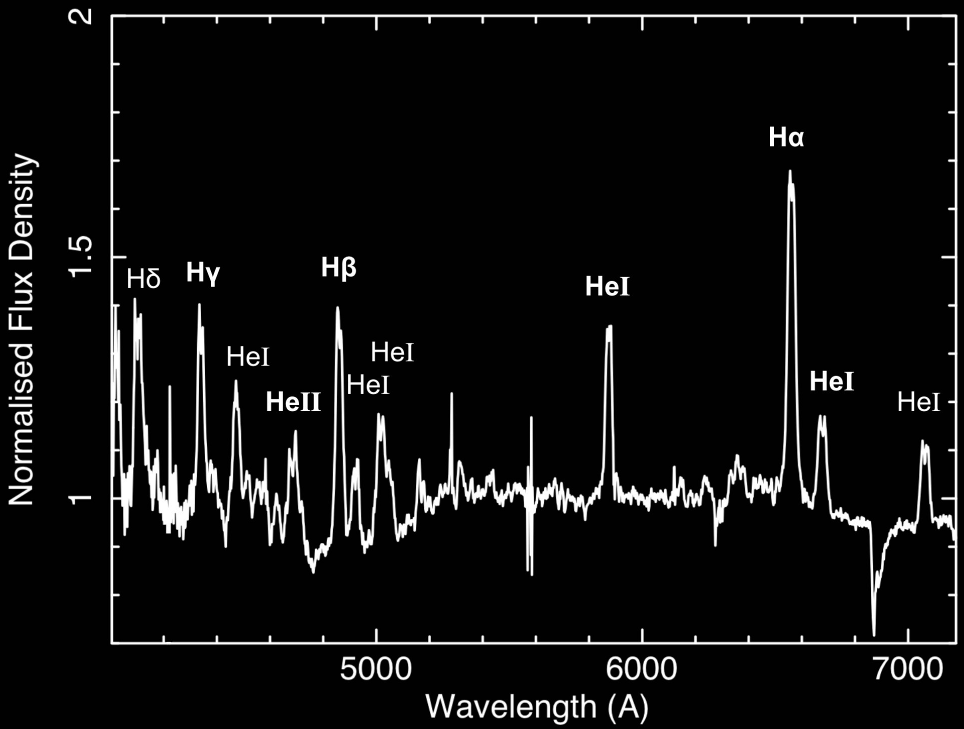

Messa+2026 in press

AVERAGE SPECTRUM

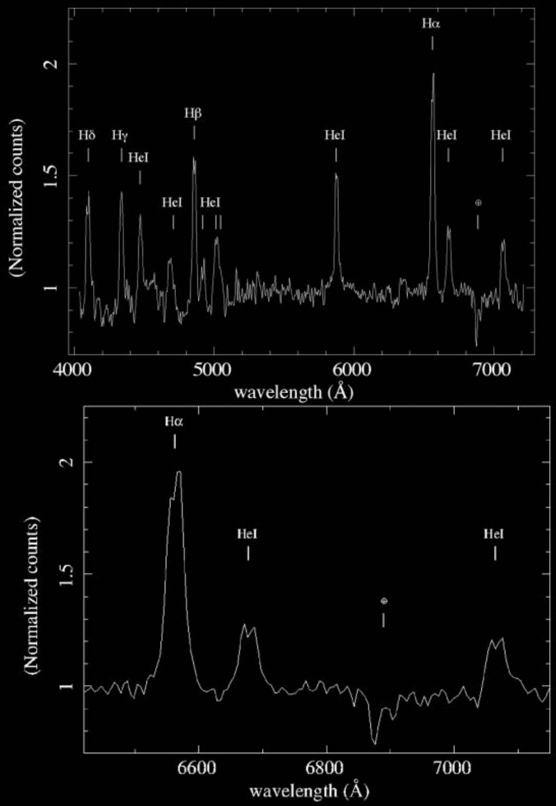

Coti Zelati+, 2014

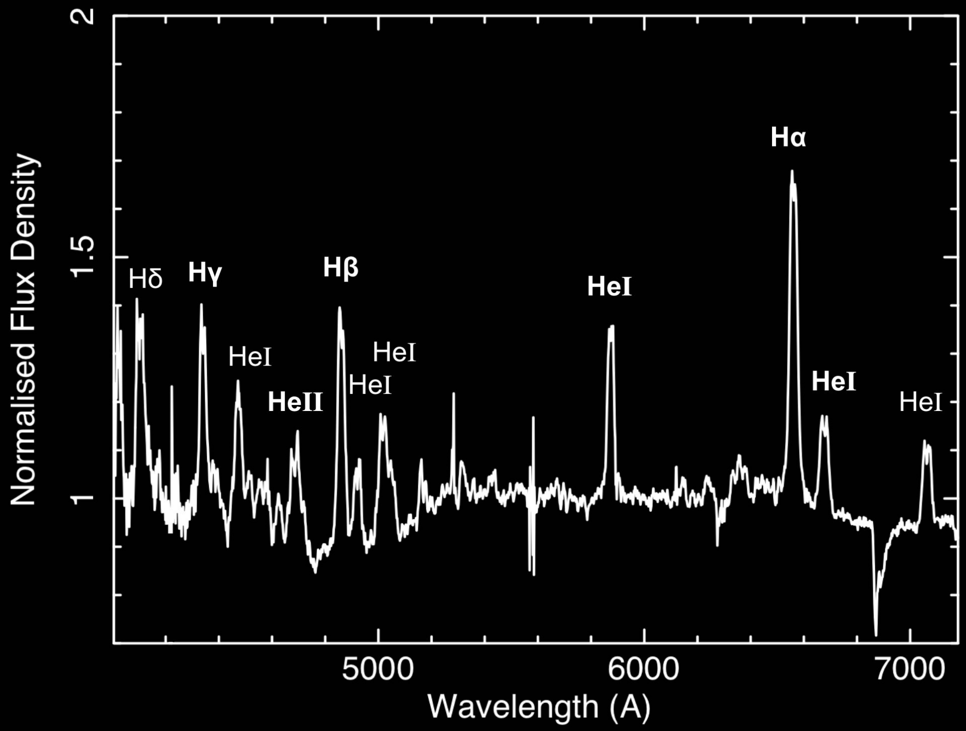

Messa+2026 in press

EMISSION LINE VARIABILITY

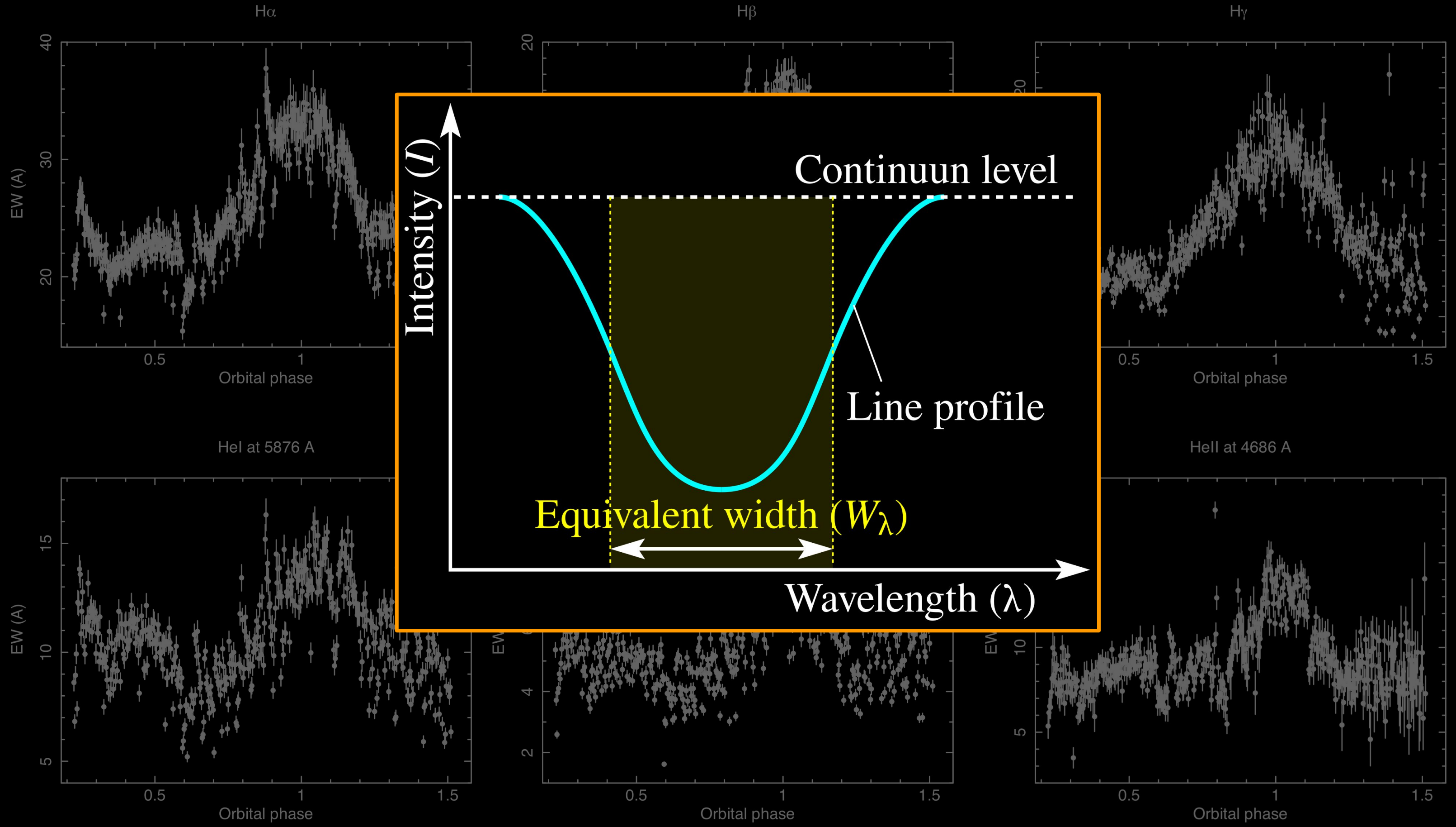

EMISSION LINE VARIABILITY

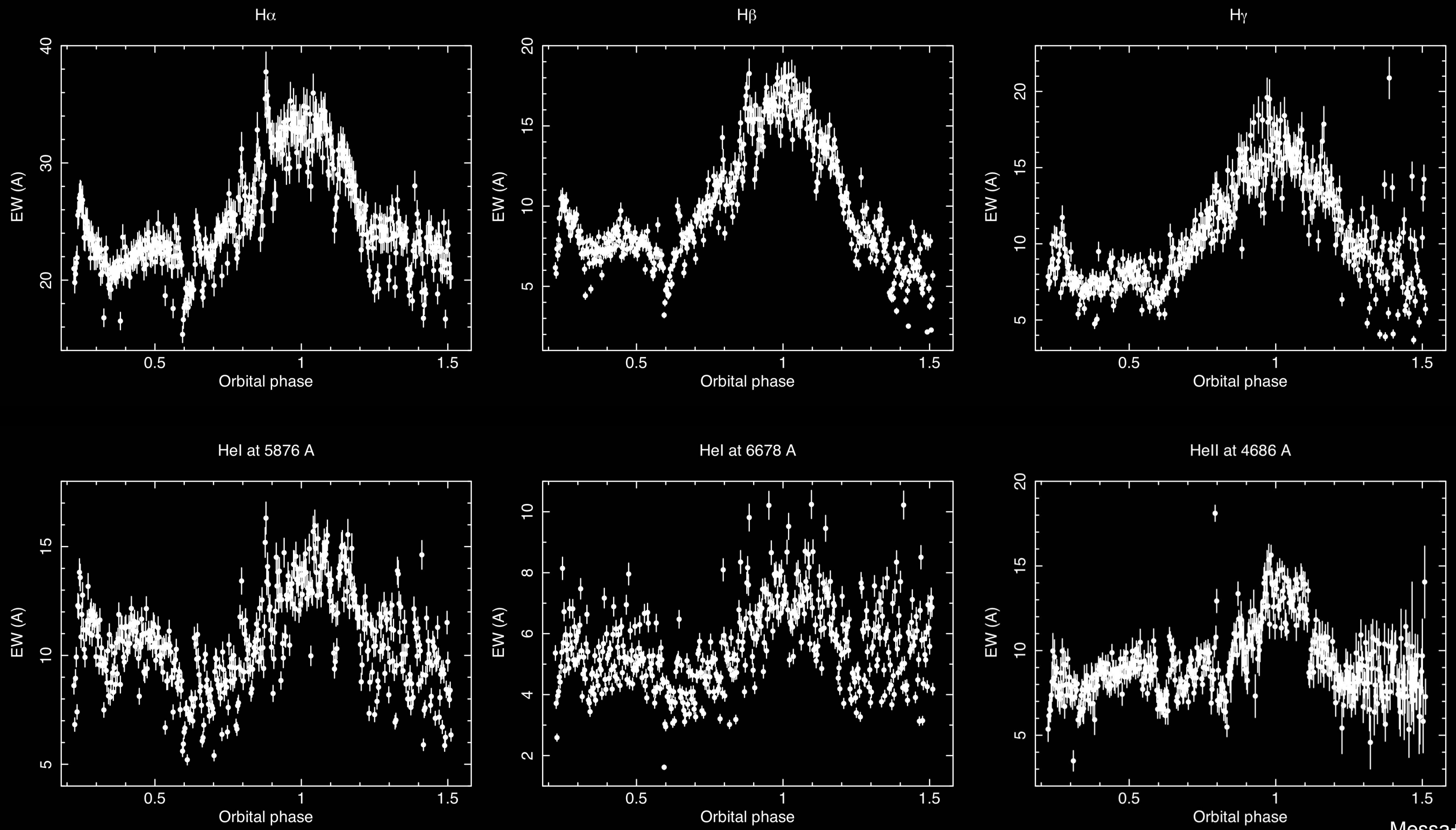

Messa+2026, in press

EMISSION LINE VARIABILITY

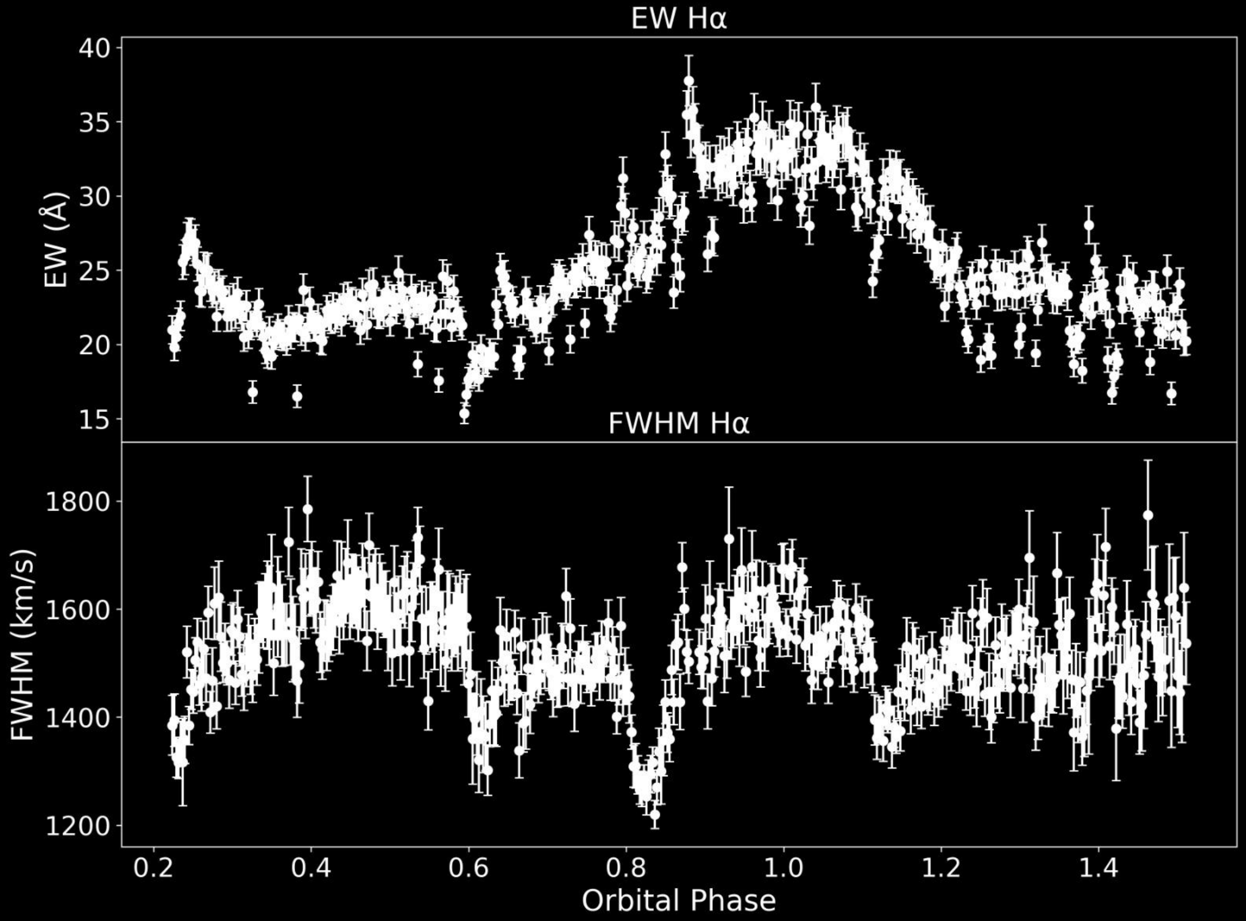

Messa+2026, in press

EMISSION LINE VARIABILITY

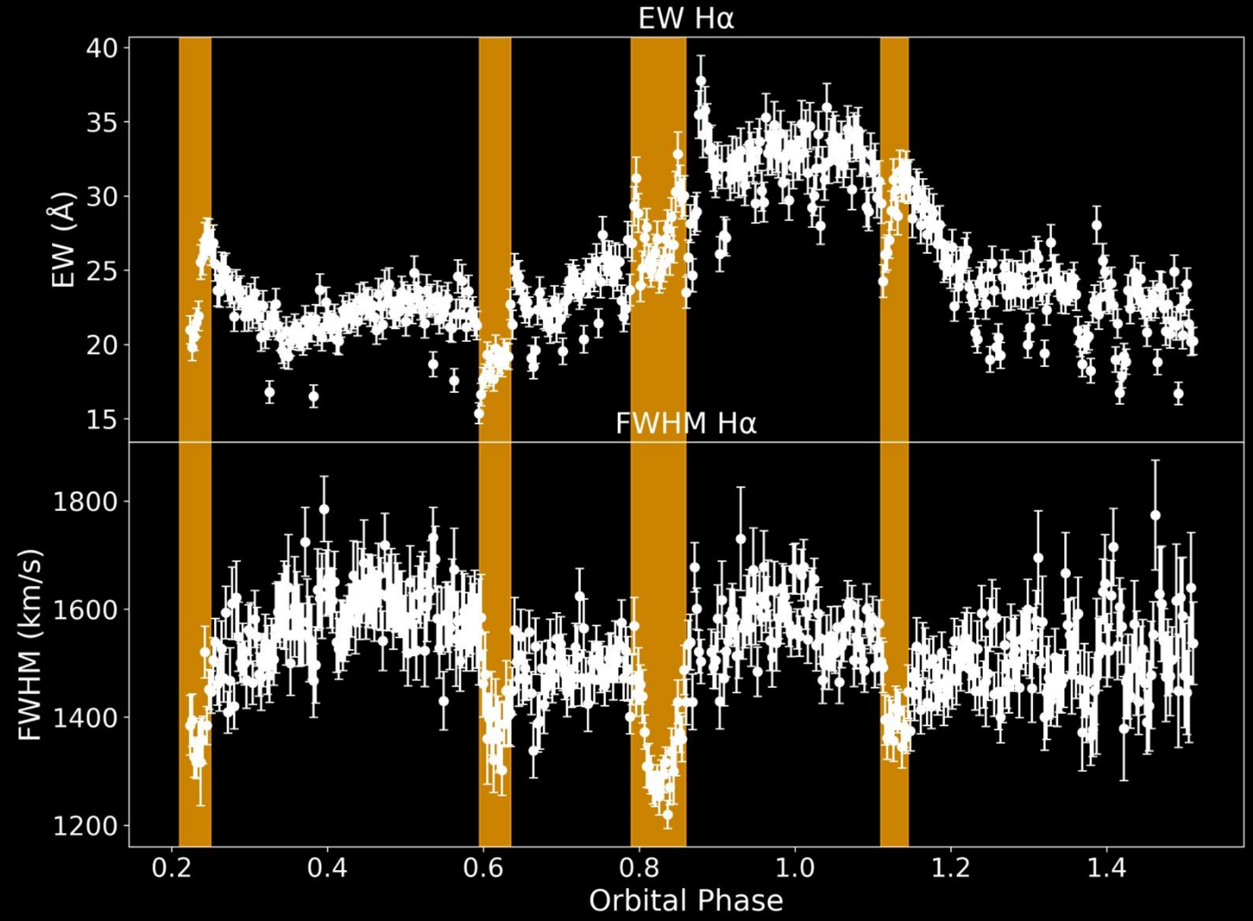

Messa+2026, in press

EMISSION LINE VARIABILITY

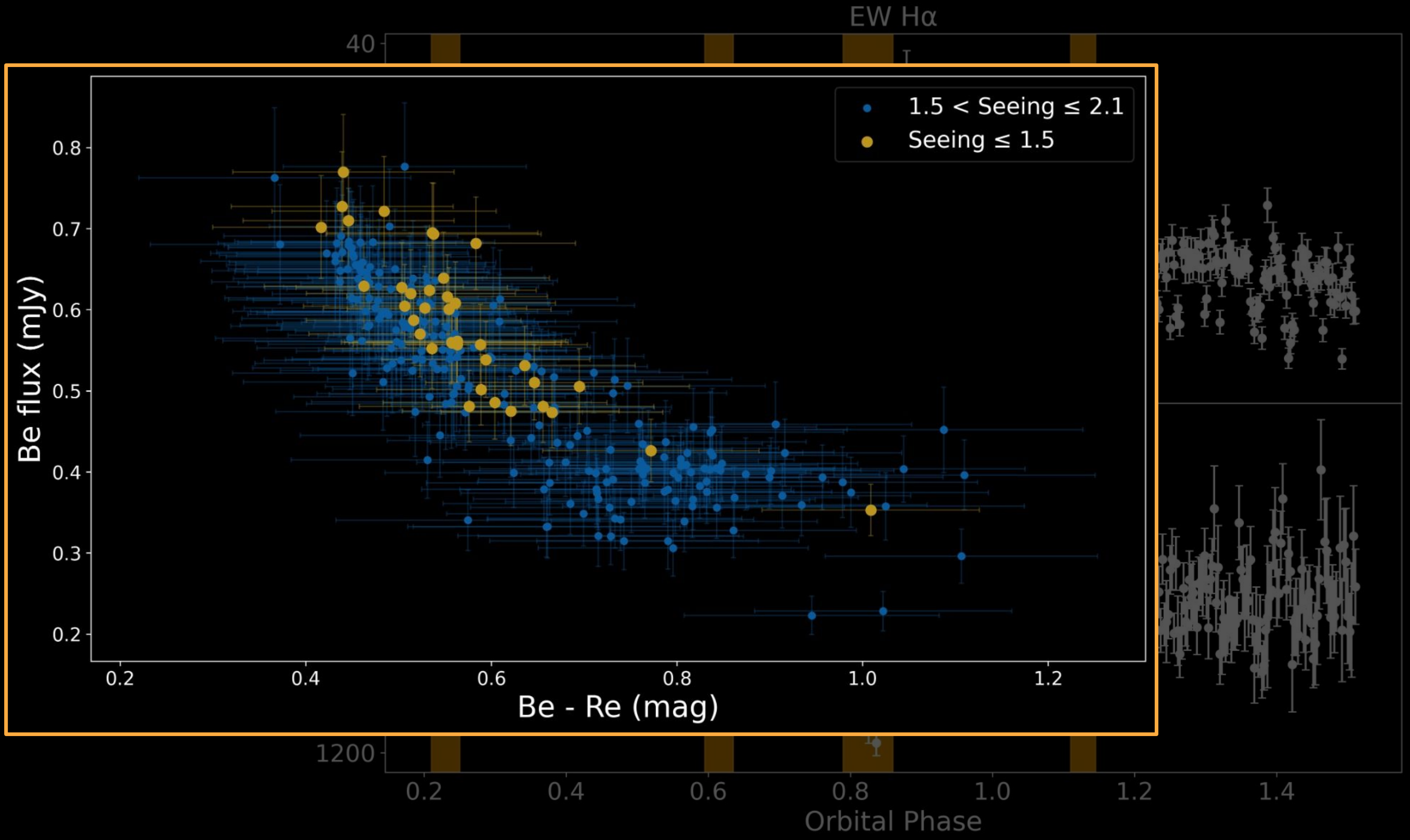

Messa+2026, in press

EMISSION LINE VARIABILITY

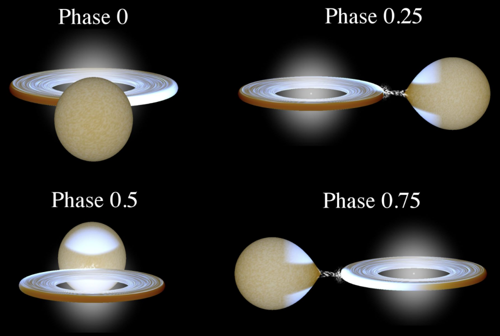

Baglio+, 2016

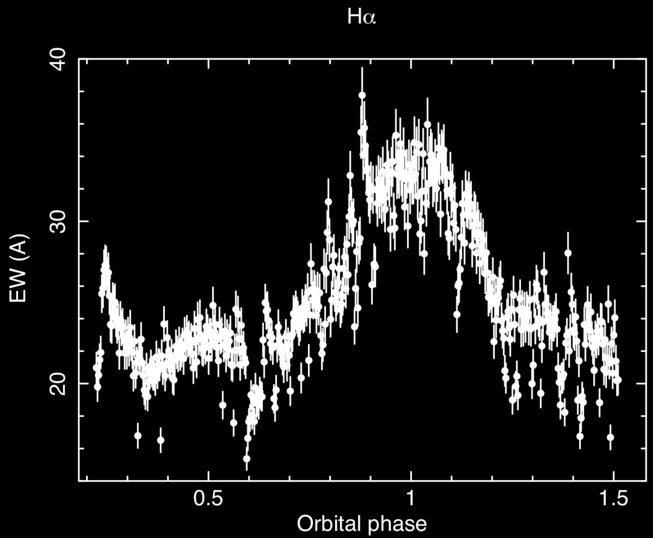

EMISSION LINE VARIABILITY

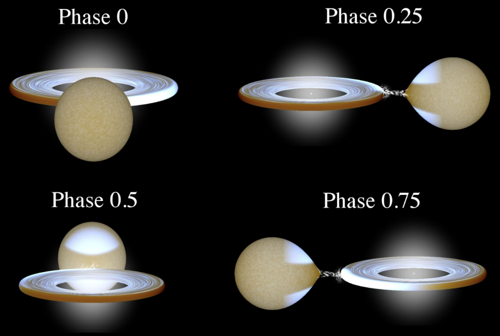

Baglio+, 2016

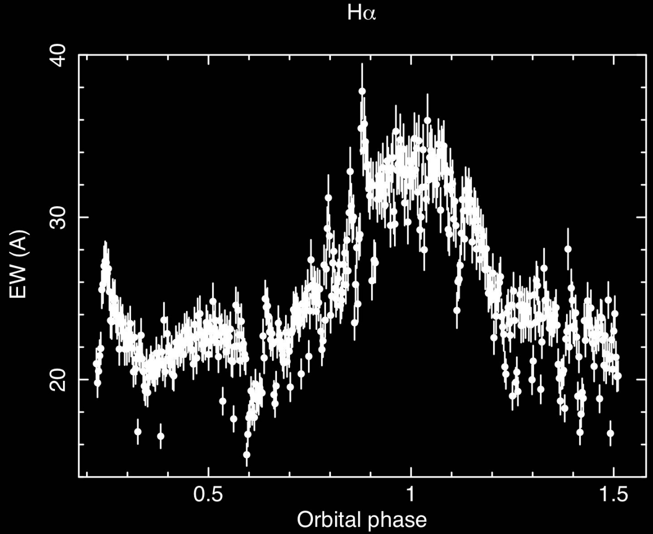

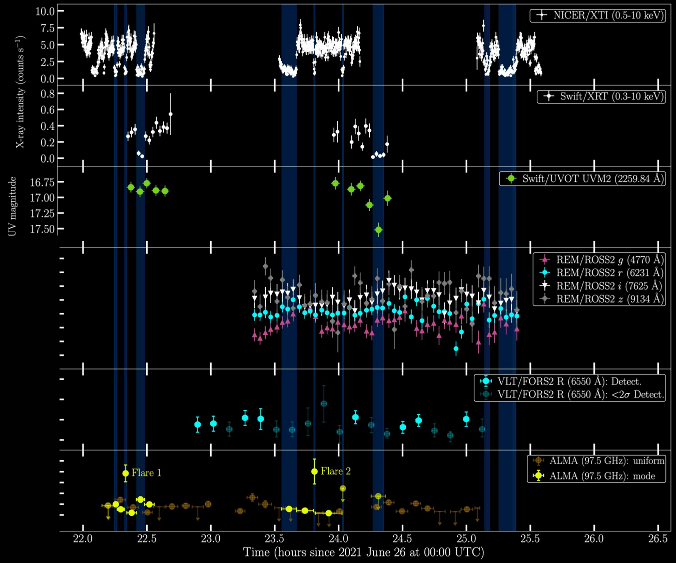

Baglio+, 2023

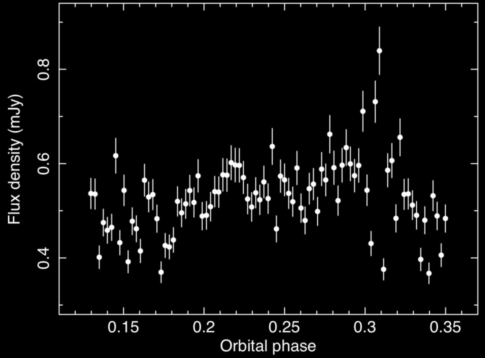

Messa+, 2024

EMISSION LINE VARIABILITY

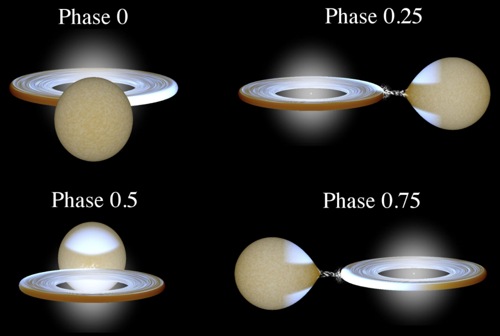

Baglio+, 2016

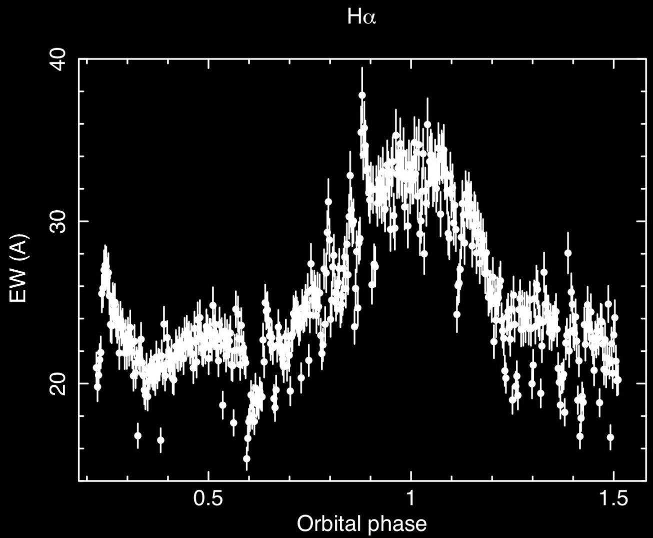

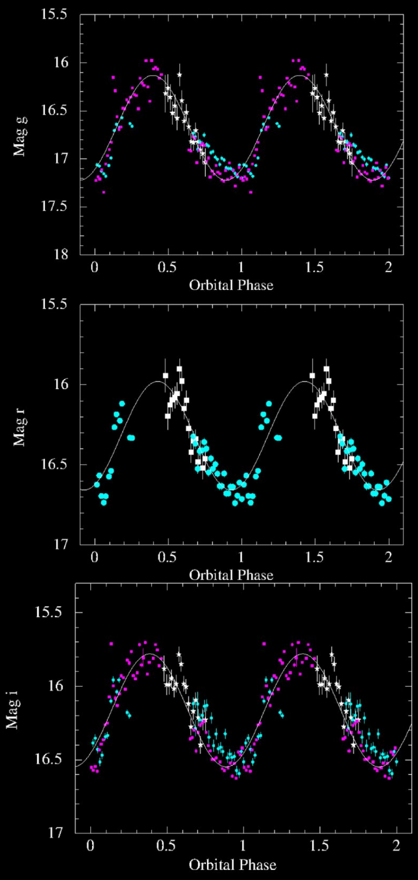

Coti Zelati+, 2014

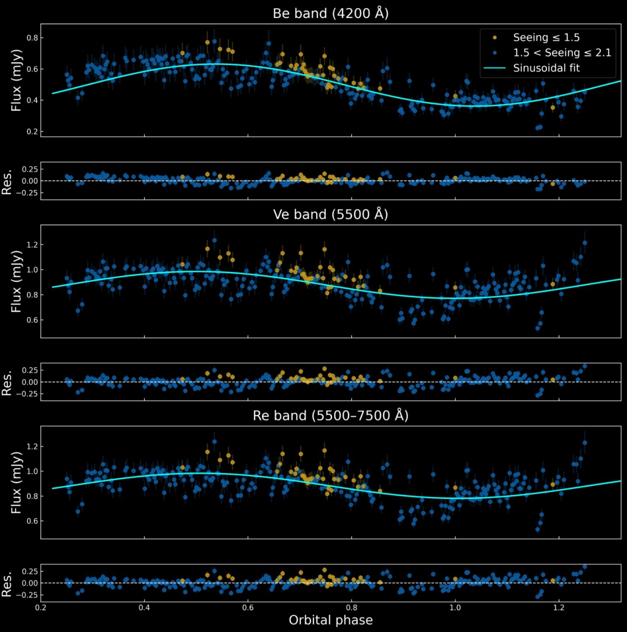

Messa+2026, in press

DOPPLER TOMOGRAPHY

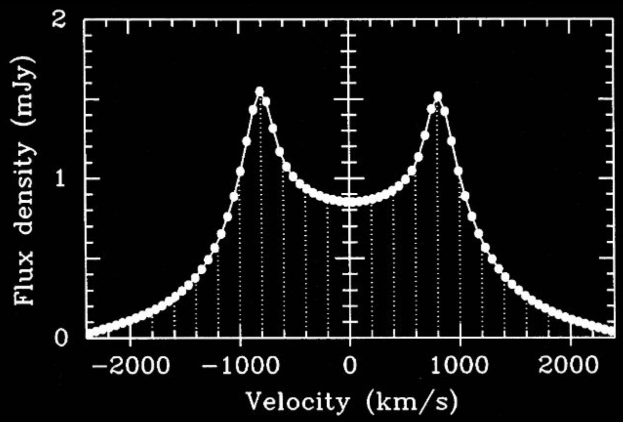

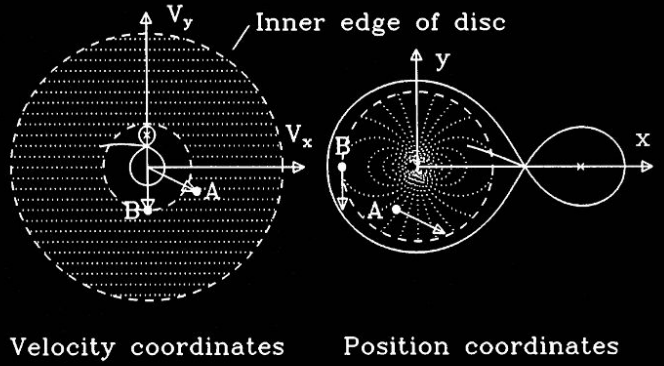

Credit: Thomas Richard Marsh

DOPPLER TOMOGRAPHY

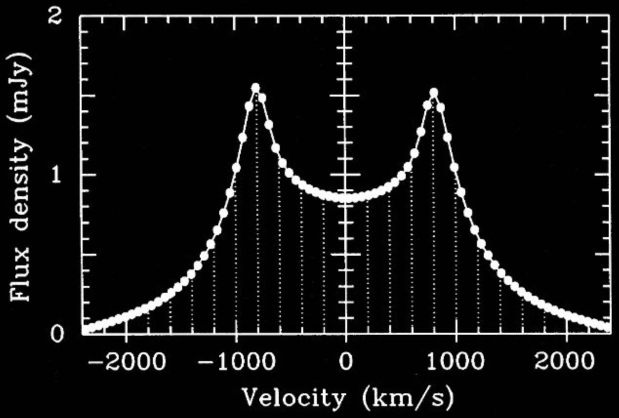

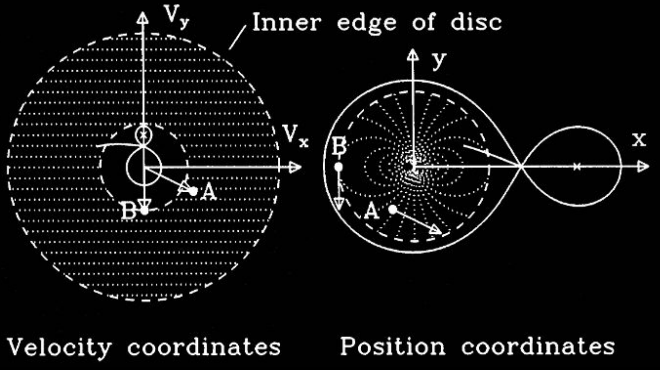

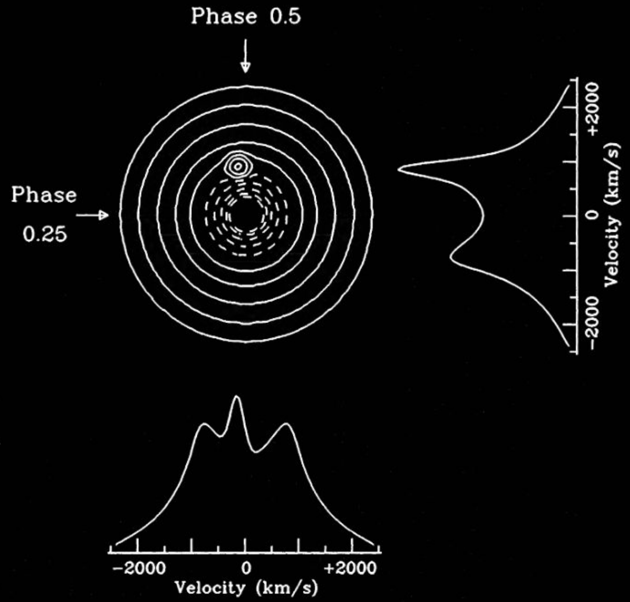

$$V_{\rm rad} = -V_x \cos\phi + V_y \sin\phi$$

Credit: Thomas Richard Marsh

DOPPLER TOMOGRAPHY

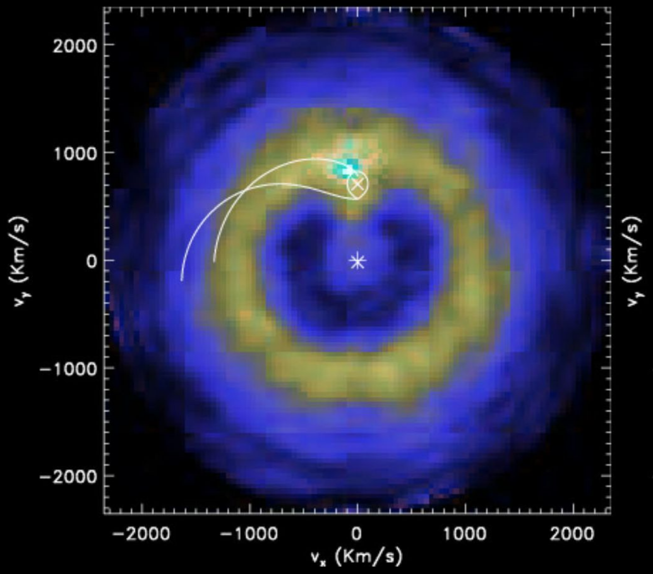

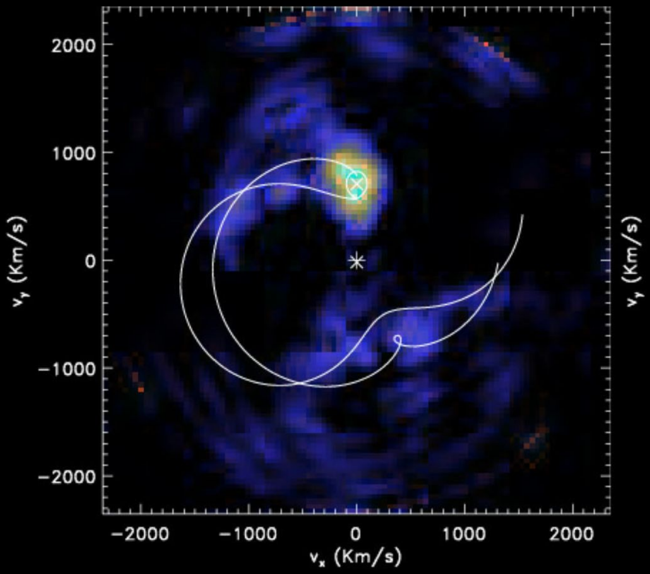

XTE J1118+480

Zurita et al., 2016

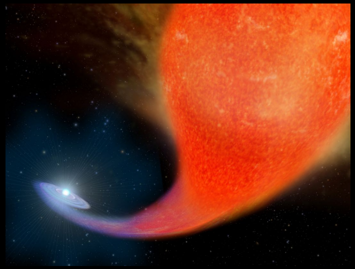

DOPPLER TOMOGRAPHY

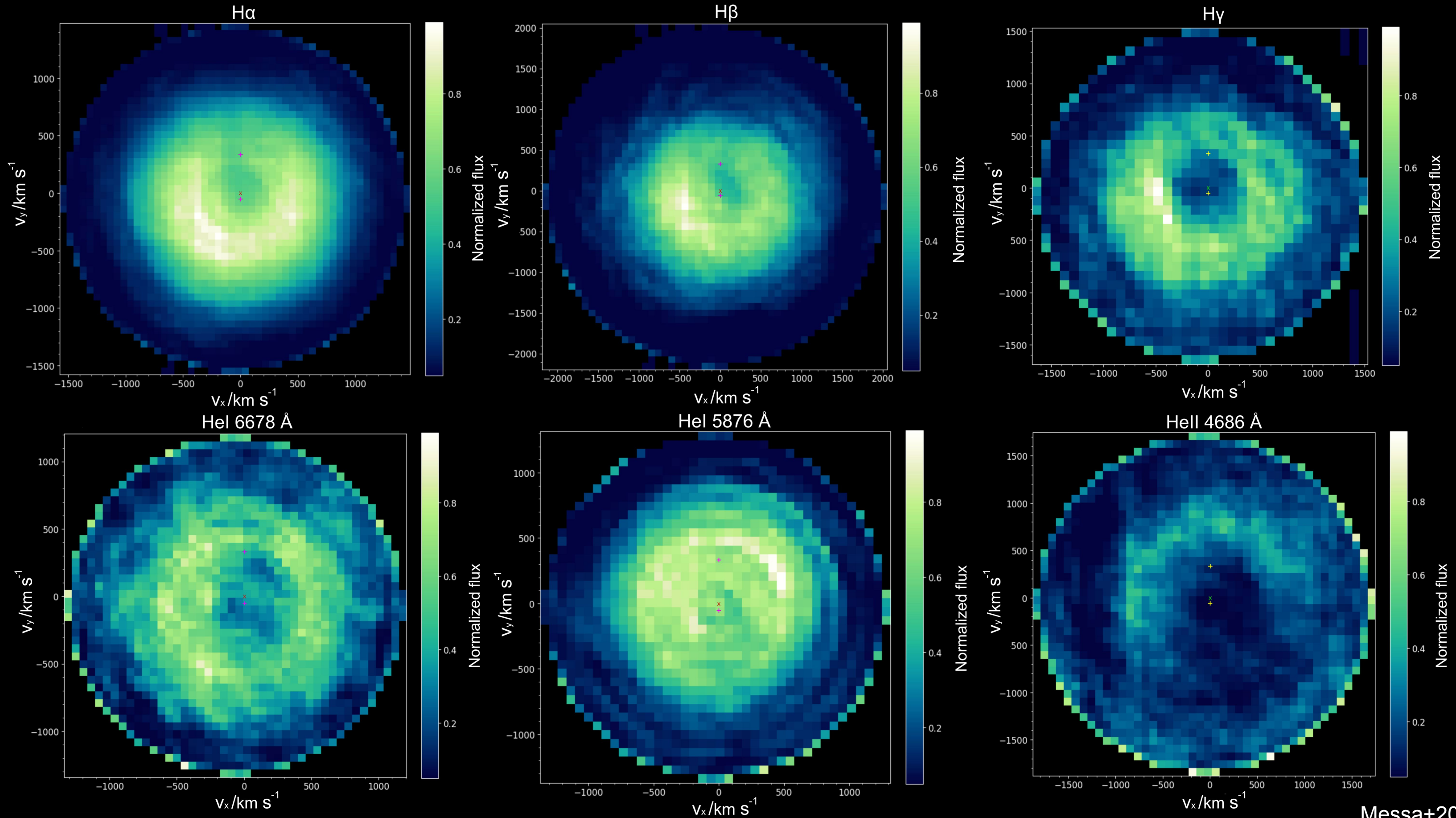

Messa+2026, in press

DOPPLER TOMOGRAPHY

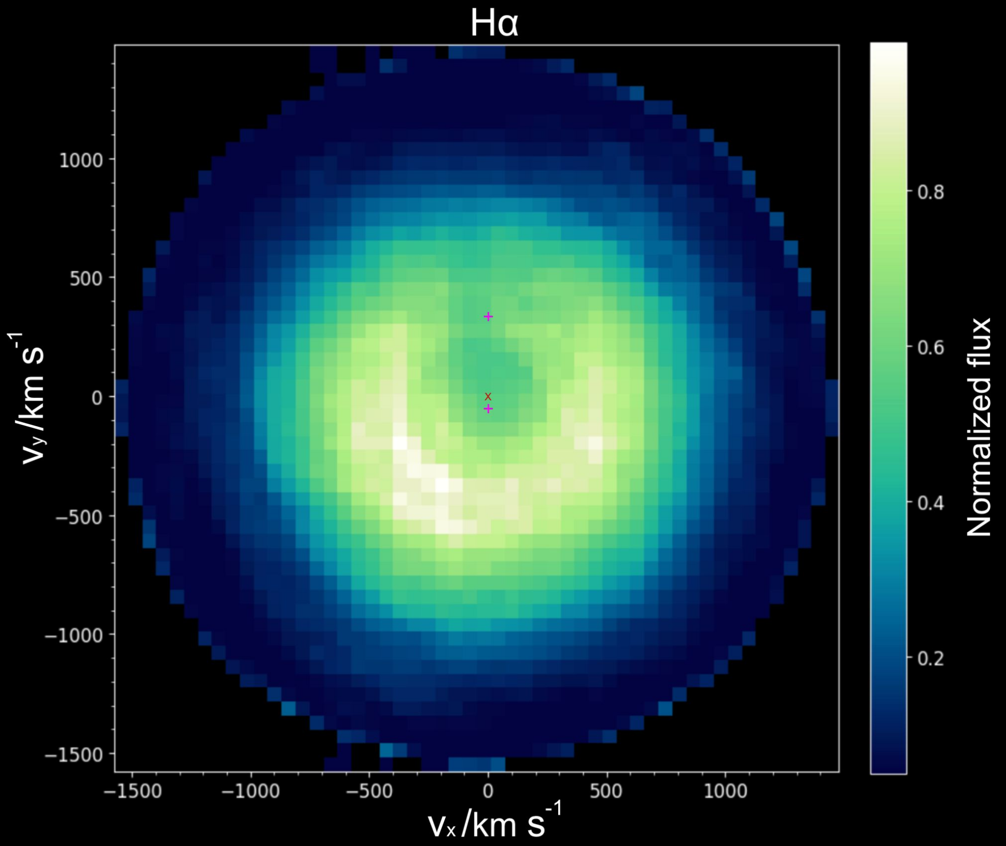

BH Lyncis

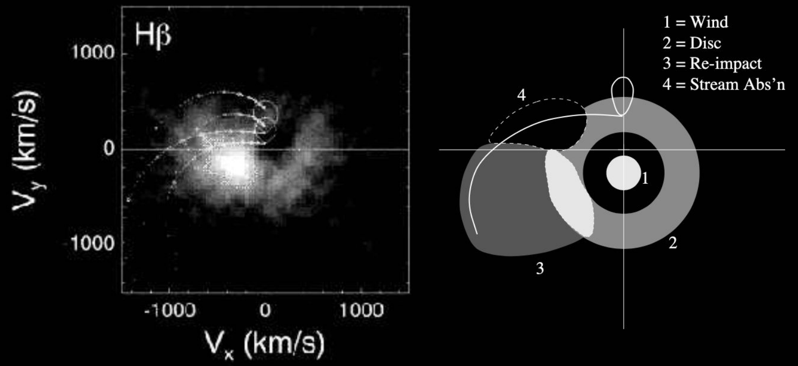

Hellier+, 2000

FUTURE PERSPECTIVES

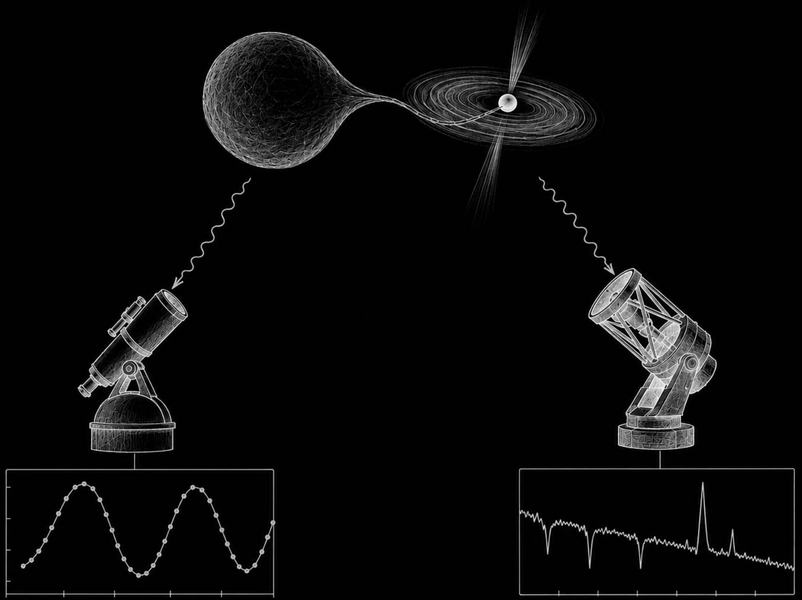

FUTURE PERSPECTIVES

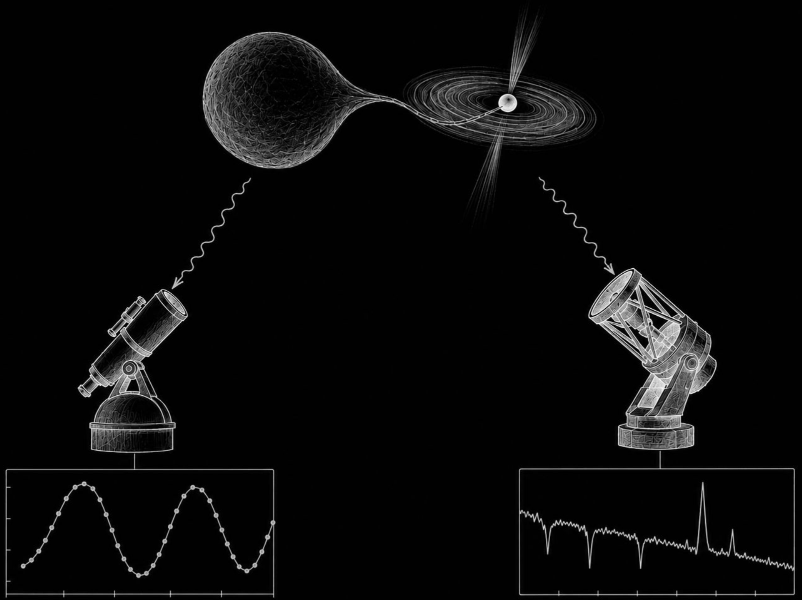

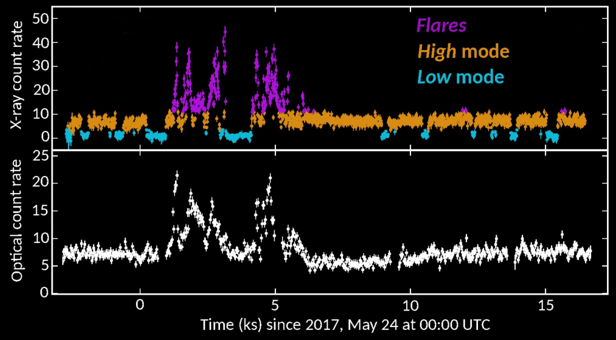

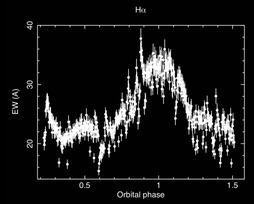

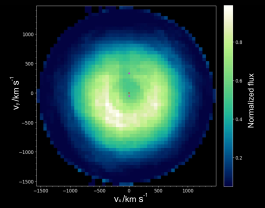

FUTURE PERSPECTIVES

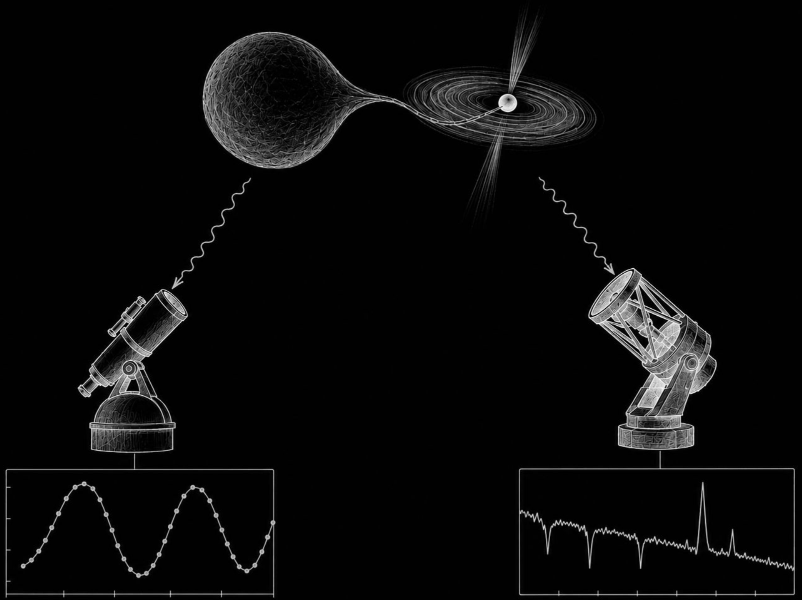

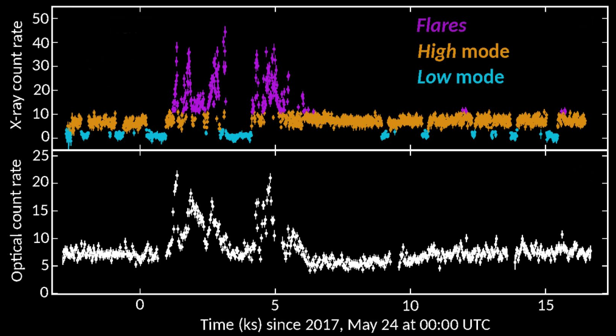

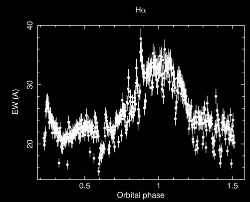

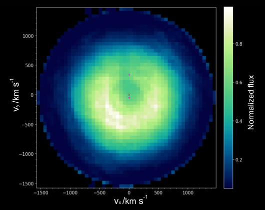

CONCLUSIONS

High time-resolution optical spectroscopy of PSR J1023+0038

Minute-timescale variability in the main emission lines

EW and FWHM variations suggest changes in the inner accretion disc

Doppler maps reveal asymmetric emission structures

Possible evidence for outflowing material

Simultaneous multiwavelength observations are key to linking spectroscopy and mode switching

THANKS FOR YOUR ATTENTION

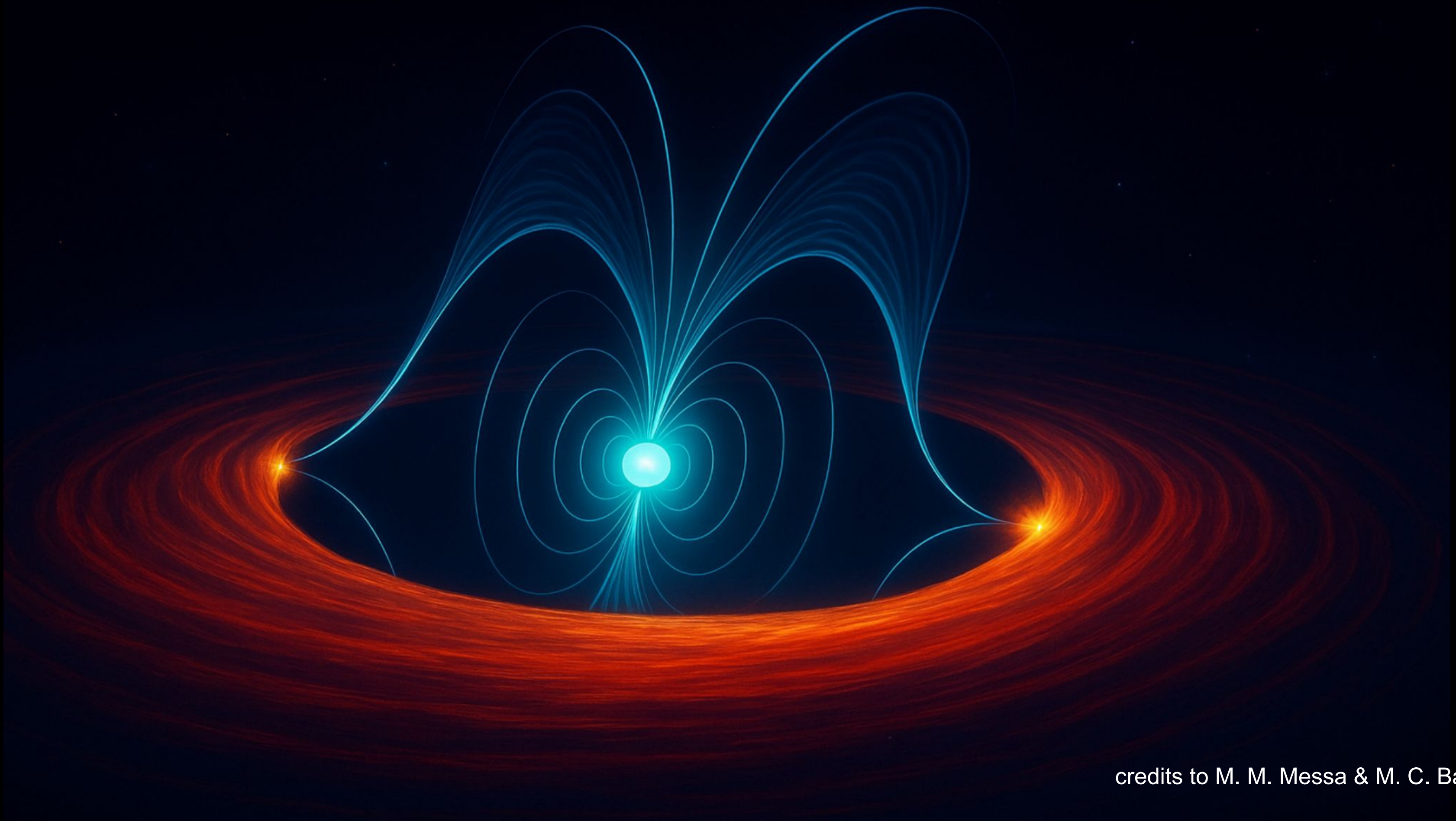

credits to M. M. Messa & M. C. Baglio

BACKUP SLIDES

DOPPLER TOMOGRAPHY

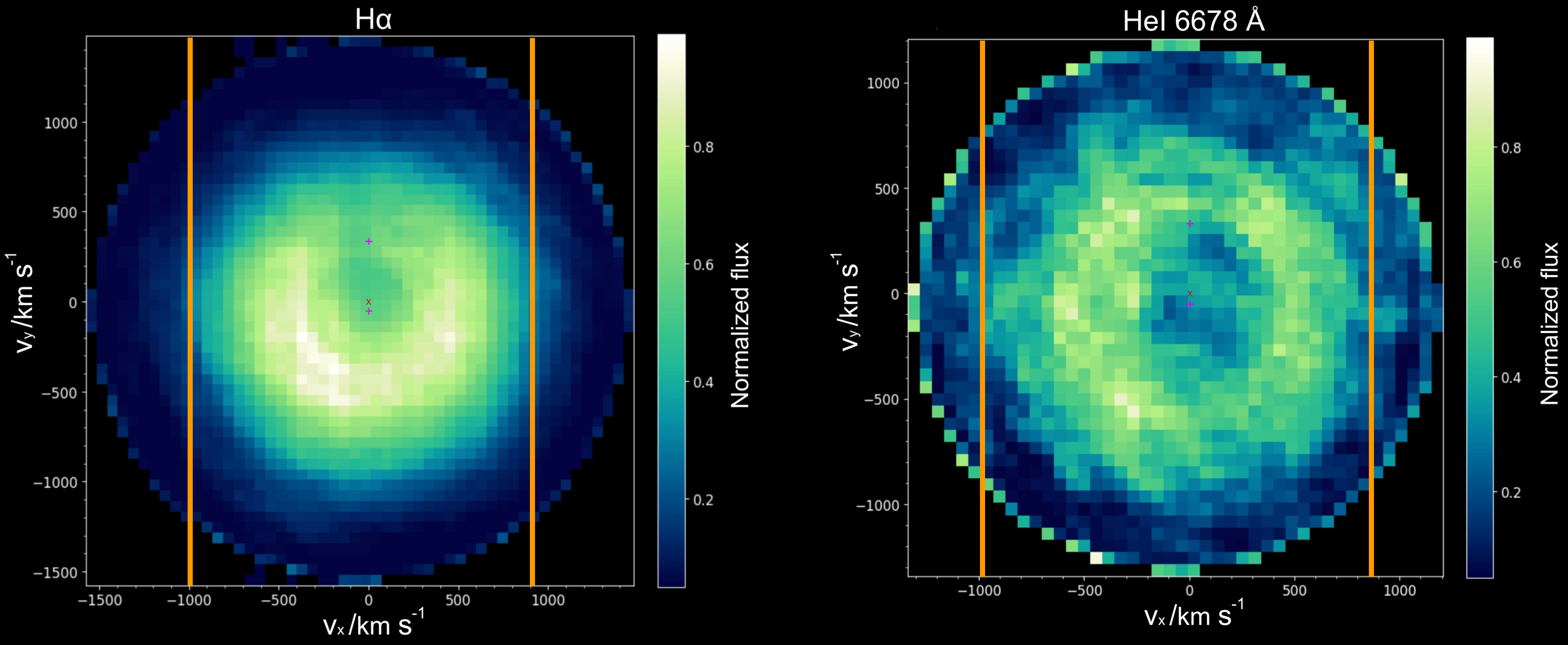

not only Keplerian!

SUB-LUMINOUS DISC STATE

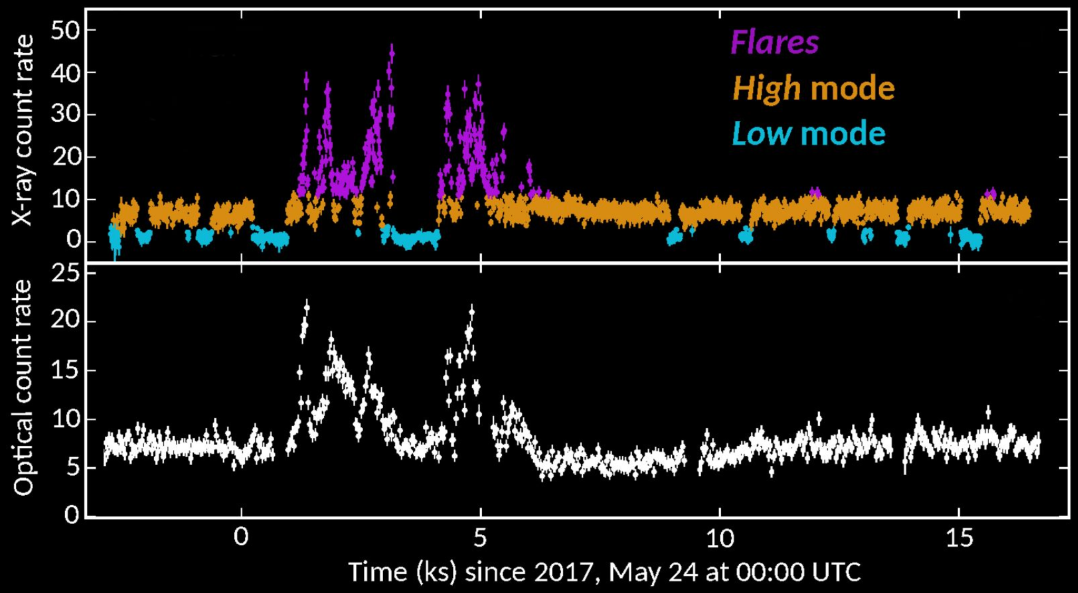

A. Papitto & de Martino, 2022

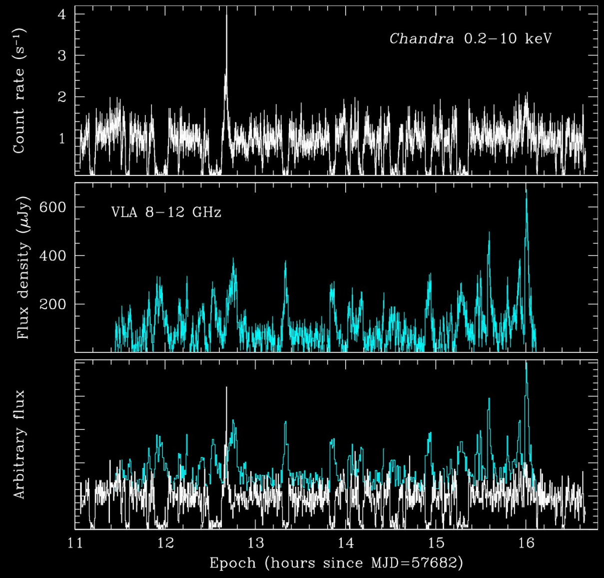

Bogdanov+, 2018

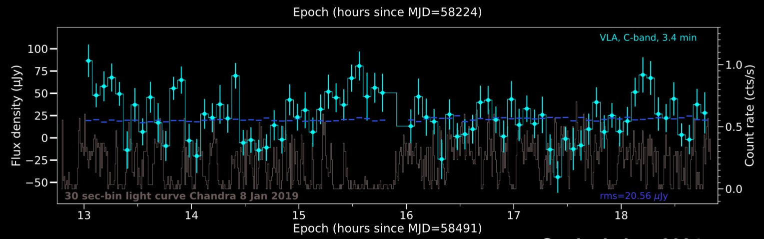

Gusinskaia+, 2024

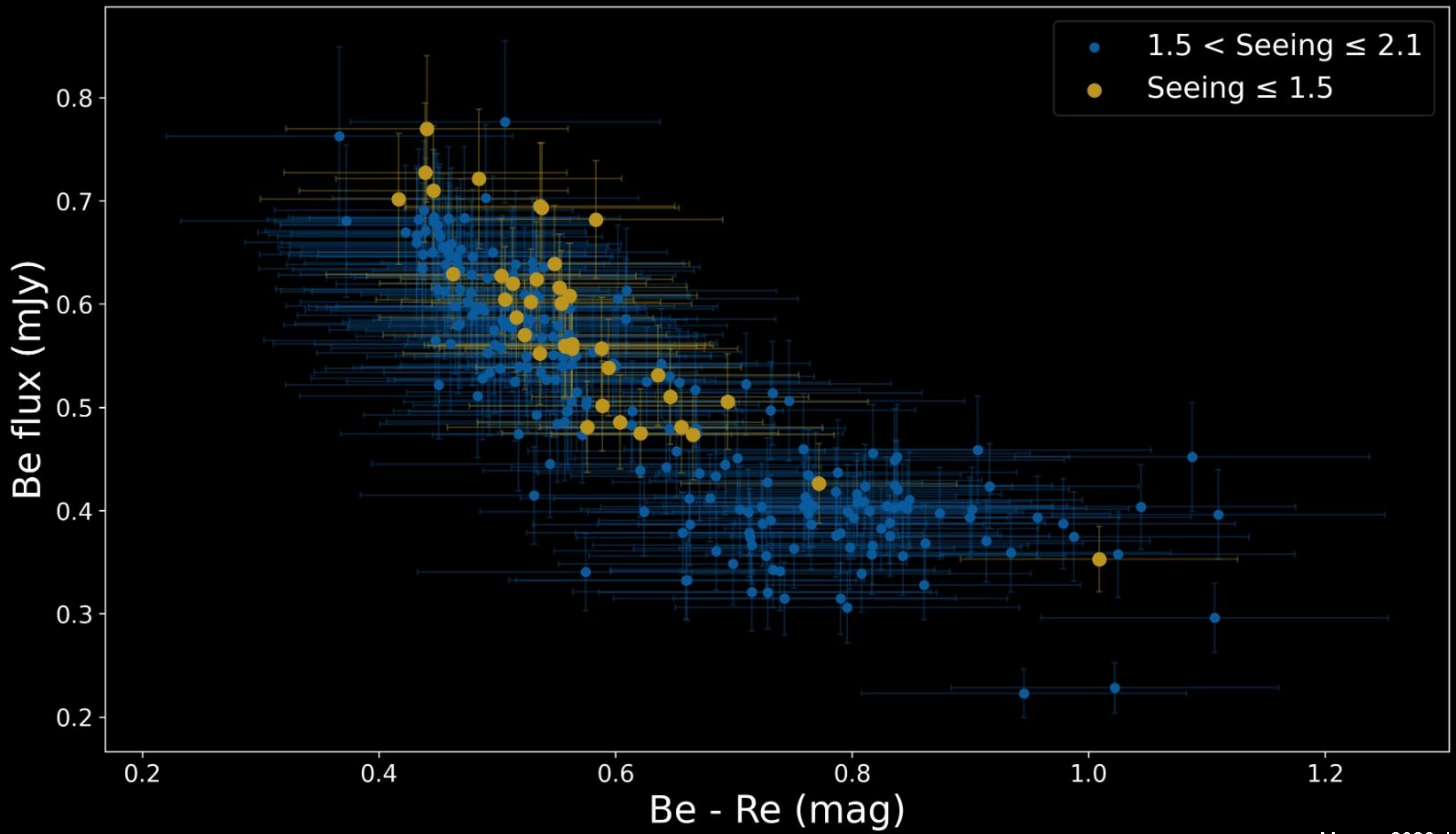

Messa+2026, in press

Be band continuum residuals

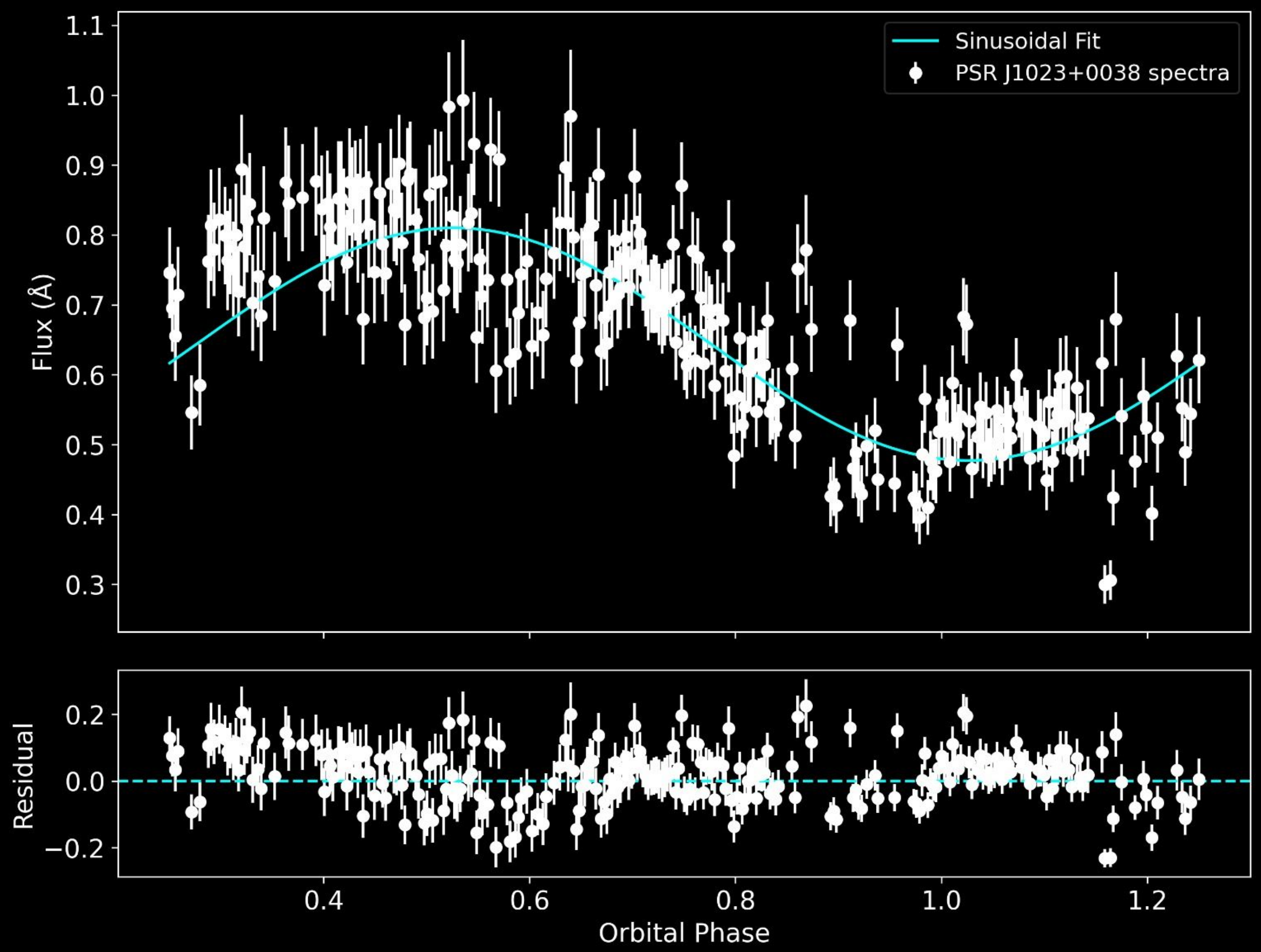

M. M. Messa

Hα

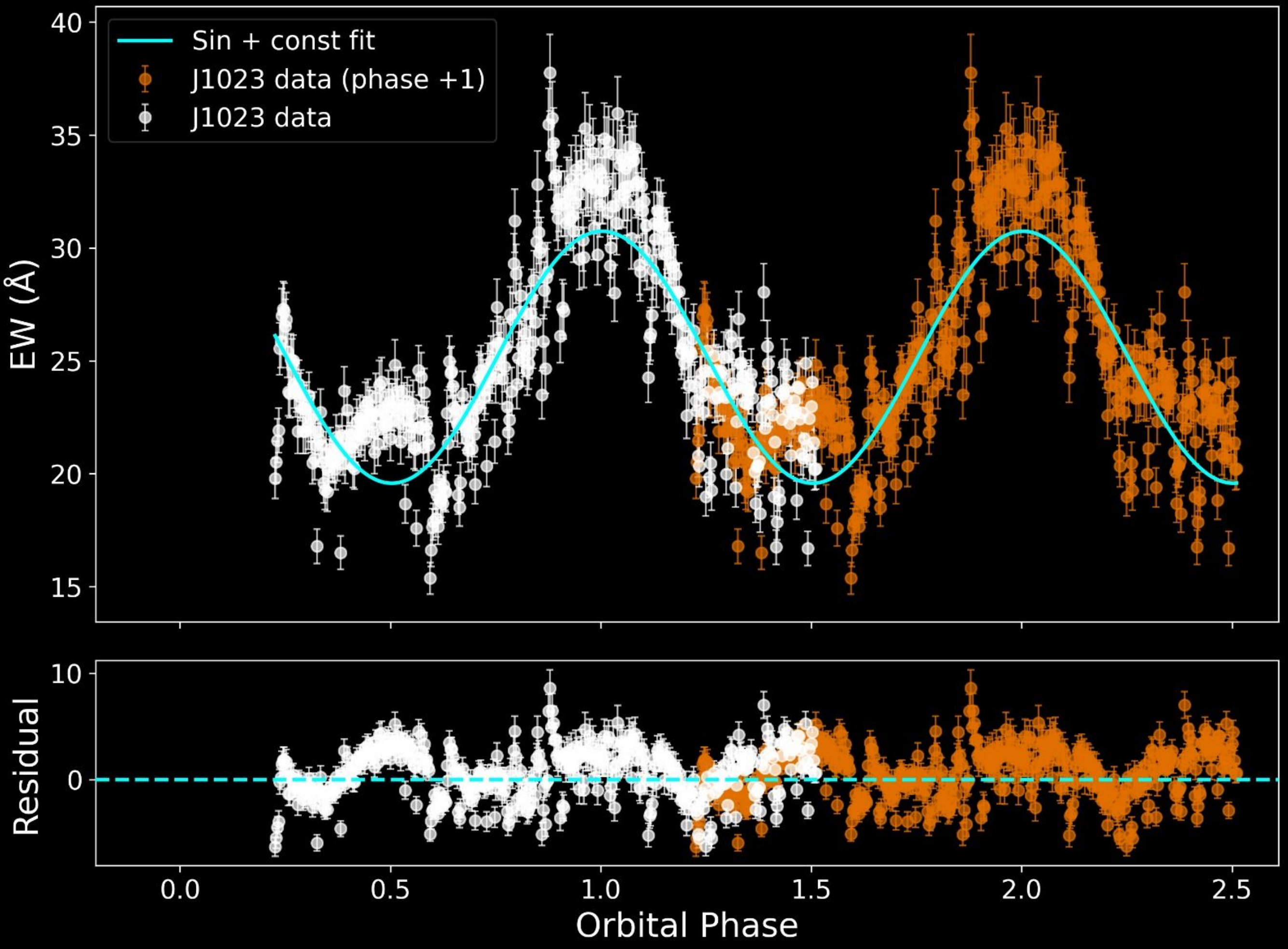

Messa+2026, in press

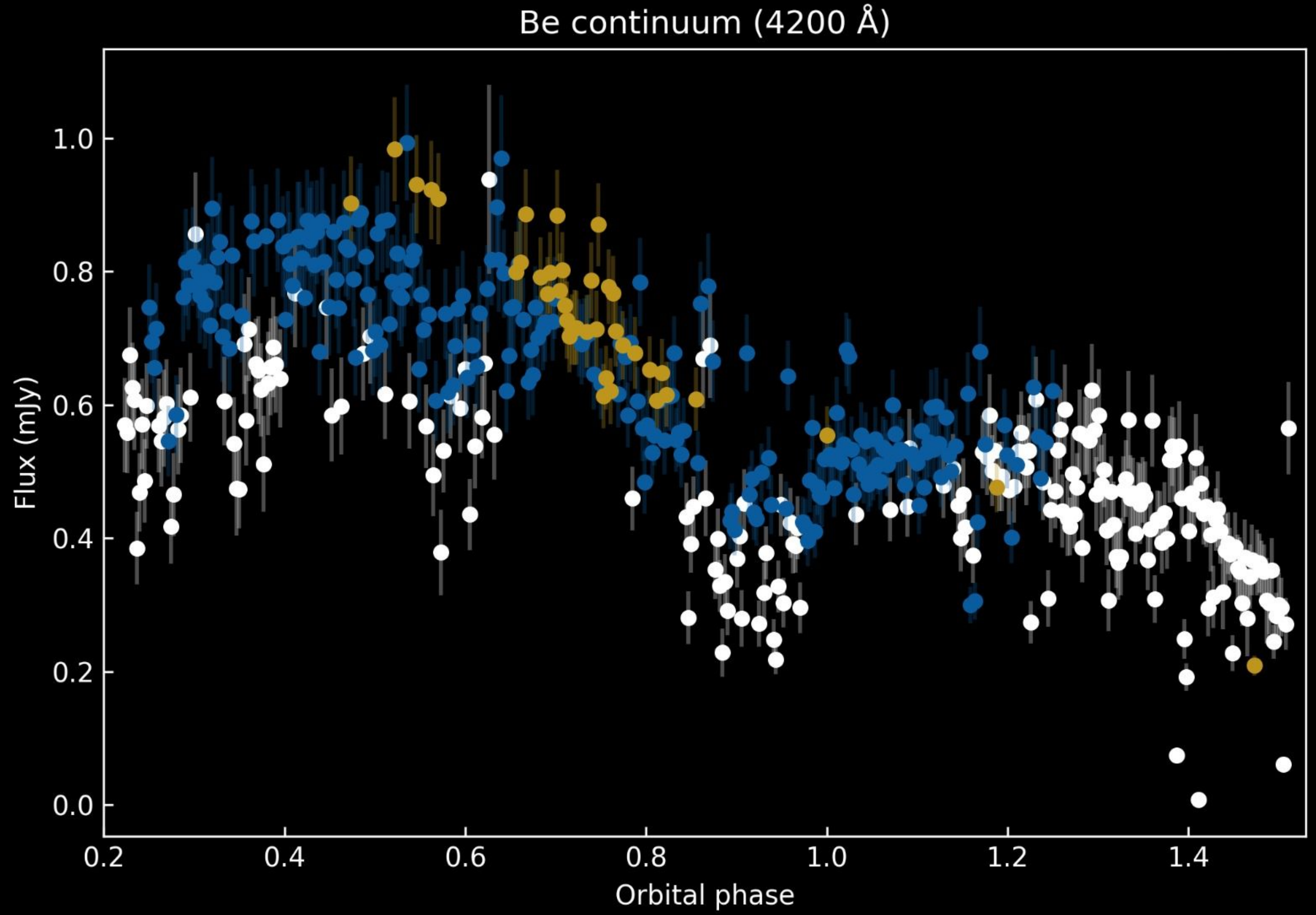
Be continuum (4200 Å)
Flux (mJy)
1.0
0.8
0.6
0.4
0.2
0.0
0.2
0.4
0.6
0.8
1.0
1.2
1.4
Orbital phase

M. M. Messa

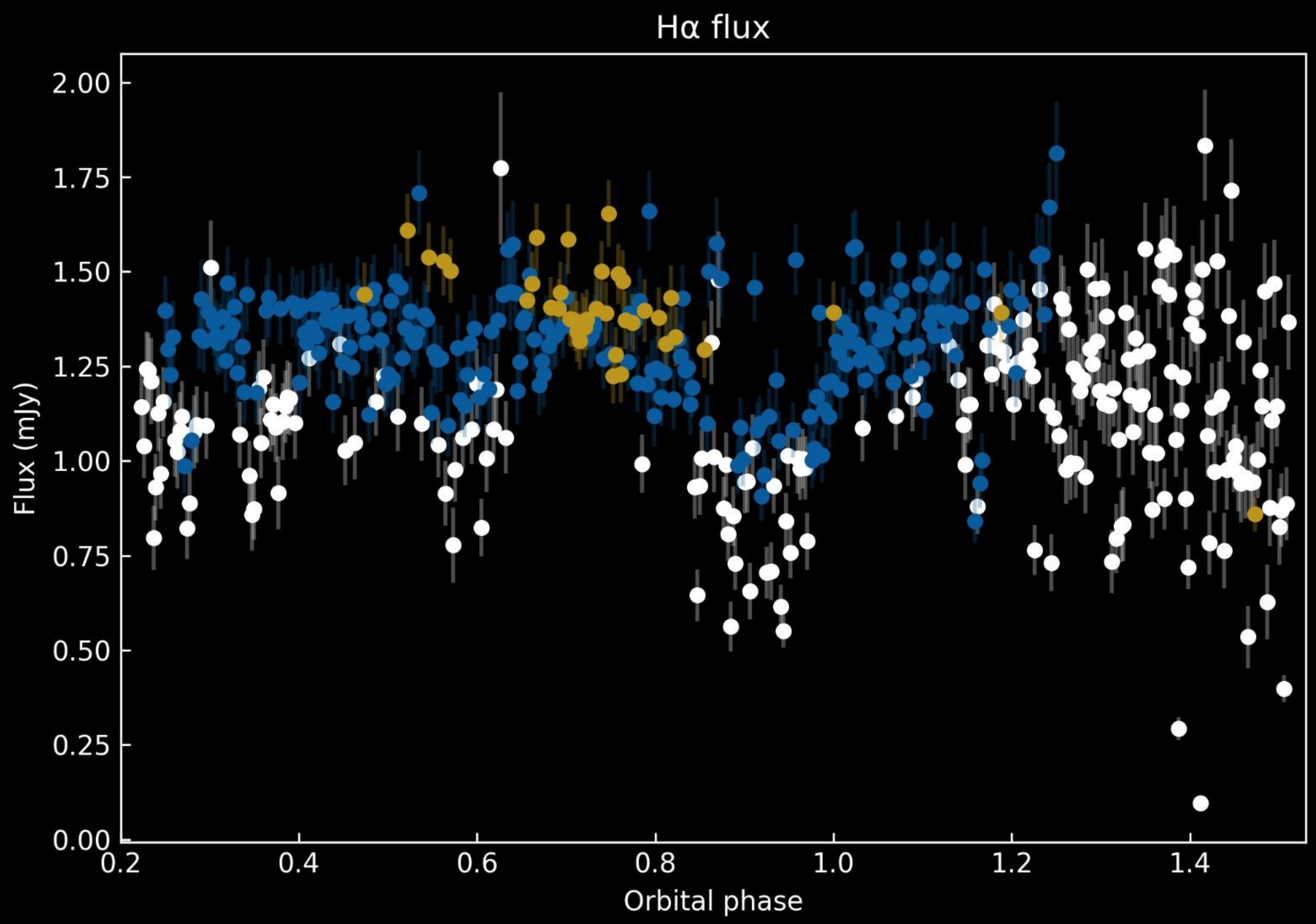

Hα flux
Flux (mJy)
2.00
1.75
1.50
1.25
1.00
0.75
0.50
0.25
0.00
0.2
0.4
0.6
0.8
1.0
1.2
1.4
Orbital phase

M. M. Messa

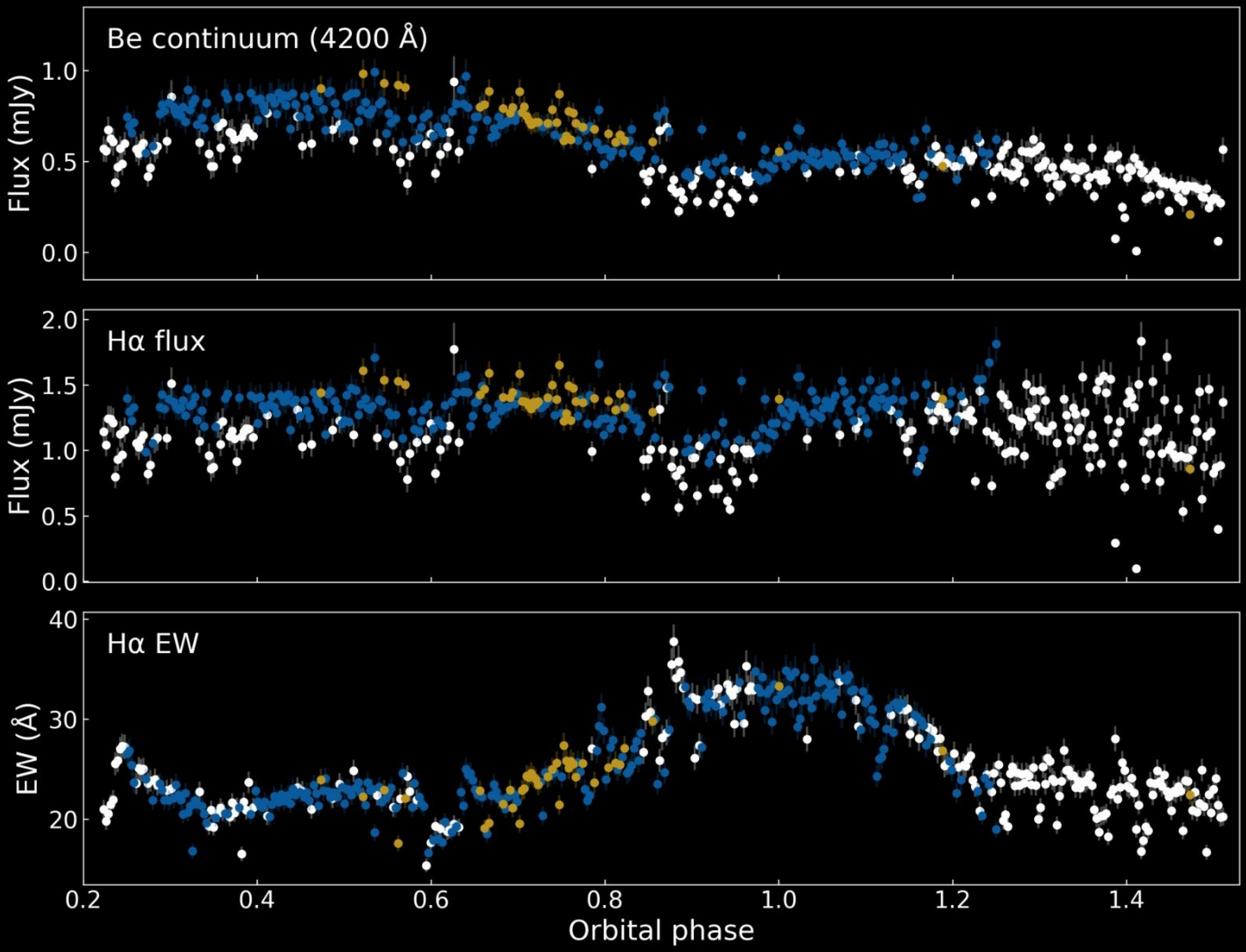

Be continuum (4200 Å)
Flux (mJy)
1.0
0.5
0.0
Hα flux
Flux (mJy)
2.0
1.5
1.0
0.5
0.0
Hα EW
EW (Å)
40
30
20
0.2
0.4
0.6
0.8
1.0
1.2
1.4
Orbital phase

M. M. Messa

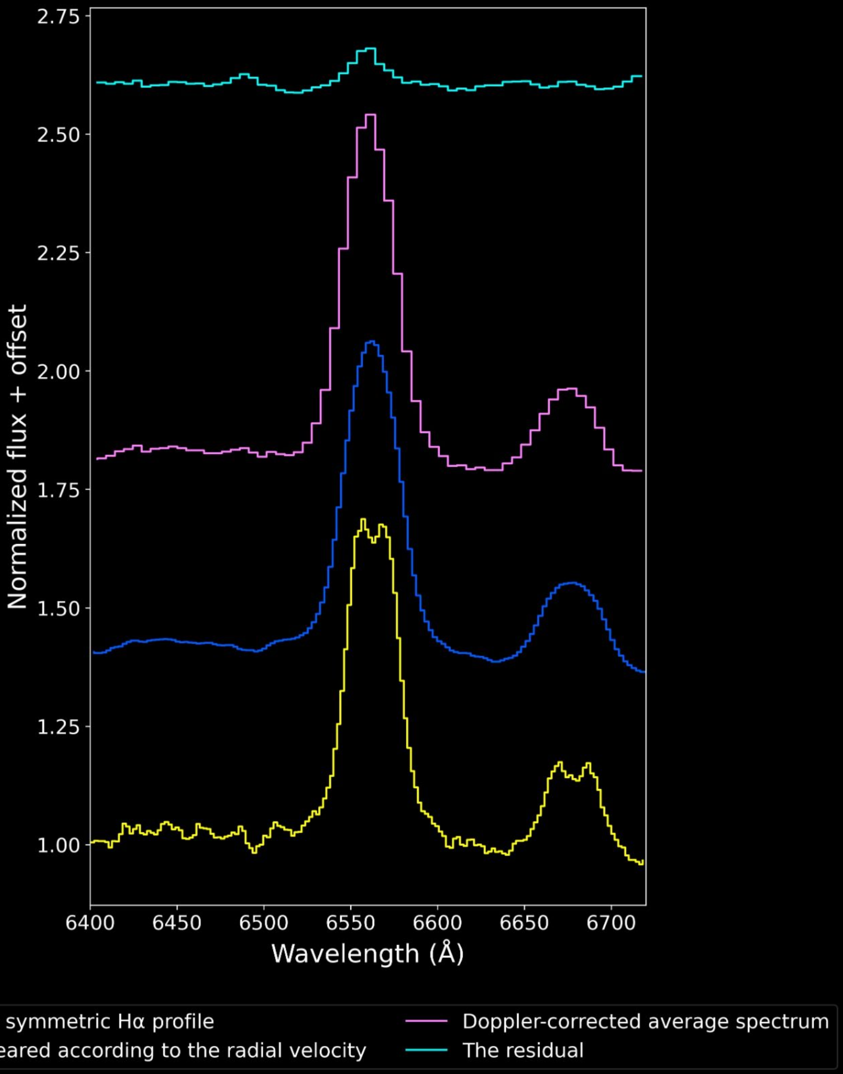

Messa+2026, in press

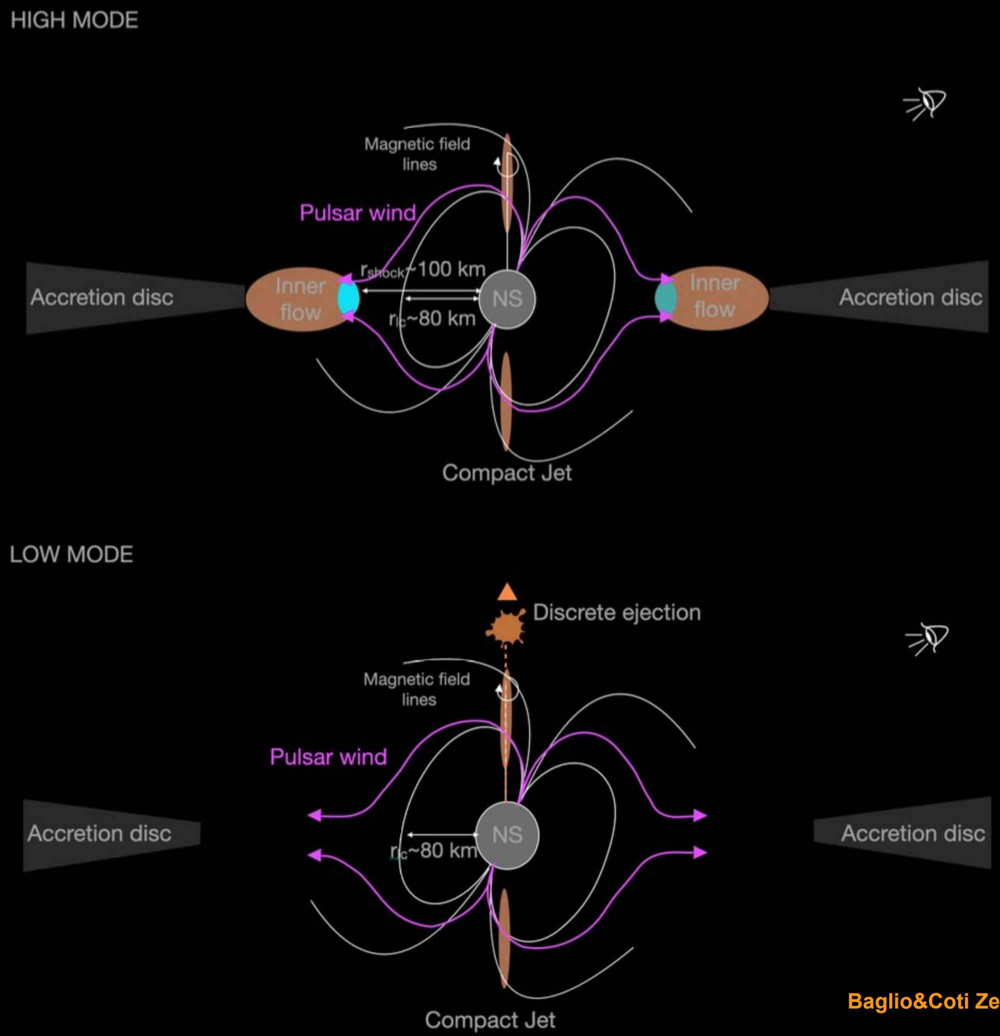

Baglio&Coti Zelati et al., 2023

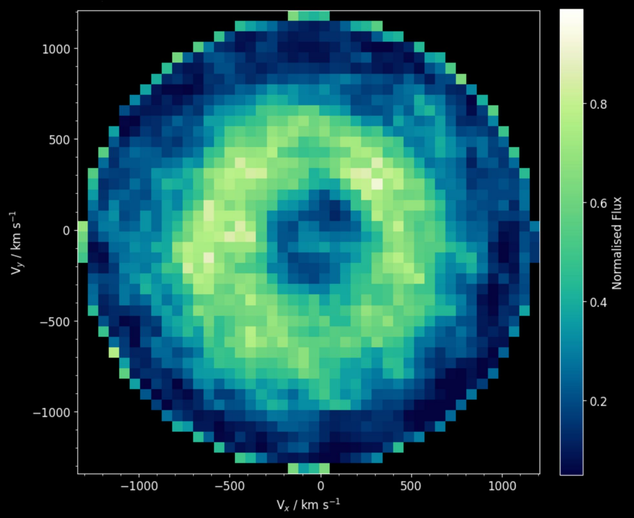

Messa et al., submitted

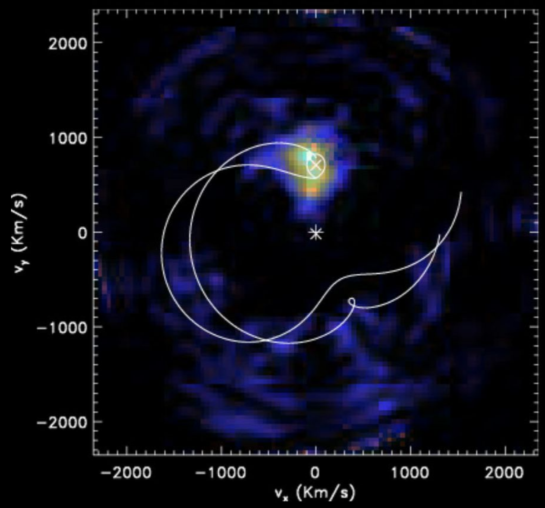

Zurita et al., 2016

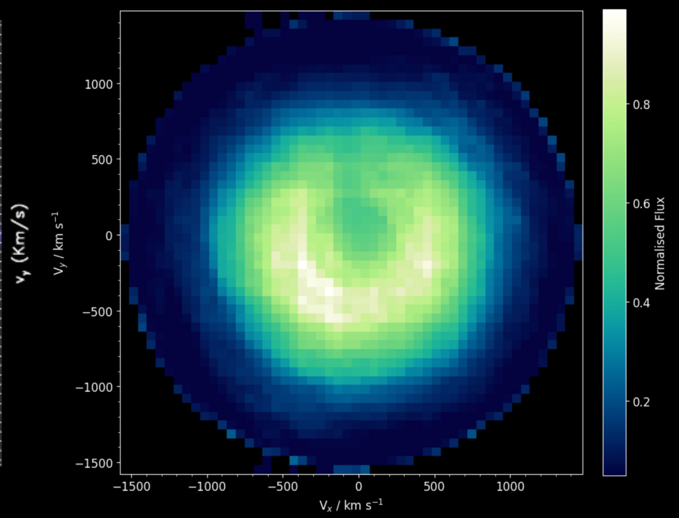

Messa et al., submitted

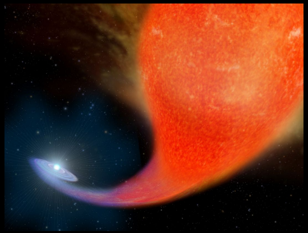

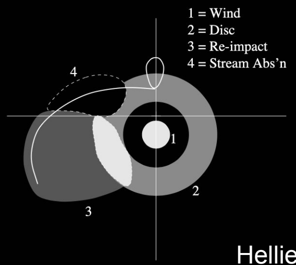

Hellier et al., 2000

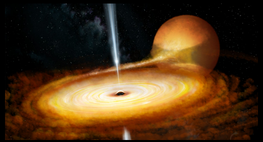

X-ray pulsar disk state

High mode
0.3-80 keV luminosity
Lx ~ 7×10^{33} erg s^{-1}

Low mode
0.3-80 keV luminosity
Lx ~ 3×10^{33} erg s^{-1}

Flaring mode
Lx~ $(2 - 7) \times 10^{34}$
erg s^{-1}

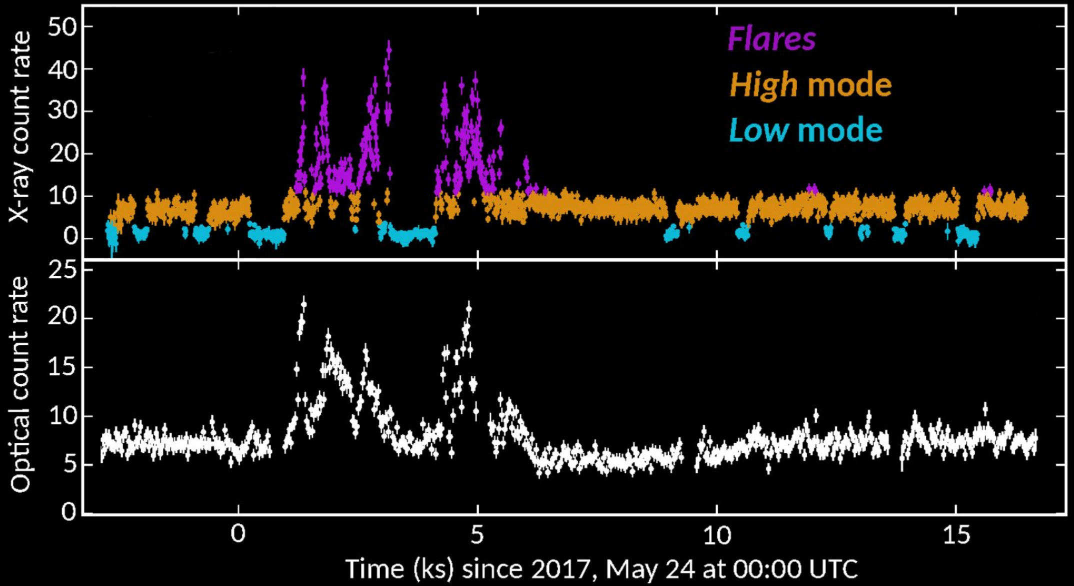

A. Papitto & de Martino, 2022

Geometry of the system

$$R_{\mathrm{lc}} = \frac{cP_{\mathrm{spin}}}{2\pi} \approx 80\ \mathrm{km}$$

radius beyond which co-rotation would be superluminal

$$R_{\mathrm{co}} = \left(\frac{GM_{\mathrm{NS}}P_{\mathrm{spin}}^2}{4\pi^2}\right)^{1/3} \approx 24\ \mathrm{km}$$

radius at which the Keplerian rotational velocity of the circumstellar material equals the rotational velocity of the star itself

$$R_{\mathrm{A}} = \mu^{4/7}(2GM_{\mathrm{NS}}\dot{M}^2)^{-1/7}$$

radius at which the magnetic field of a compact star exceeds the kinetic energy of the falling matter, disrupting the accretion disk

Geometry of the system

R_A depends on the accretion rate

If accretion proceeded to the neutron star surface

$$L_X \sim GM_{NS}\dot{M}/R_{NS}$$

$$R_A \approx 100(L_X/10^{34}\,\mathrm{erg\,s^{-1}})^{-2/7}$$

⬇

$$R_A > R_{lc}$$

does not give a consistent accretion picture

Geometry of the system

R_A depends on the accretion rate

If accretion proceeded to the neutron star surface

$$L_X \sim G M_{NS} \dot{M} / R_{NS}$$

$$R_A \approx 100 (L_X / 10^{34}\ \mathrm{erg\ s^{-1}})^{-2/7}$$

⬇

$$R_A > R_{lc}$$

for high and low mode one would find R_A/R_{lc} about 2-3

The proposed high mode

Accretion rate remains rather low

The system exhibits the high mode when the disk inner edge is outside Rlc

The disk occasionally penetrates the light cylinder

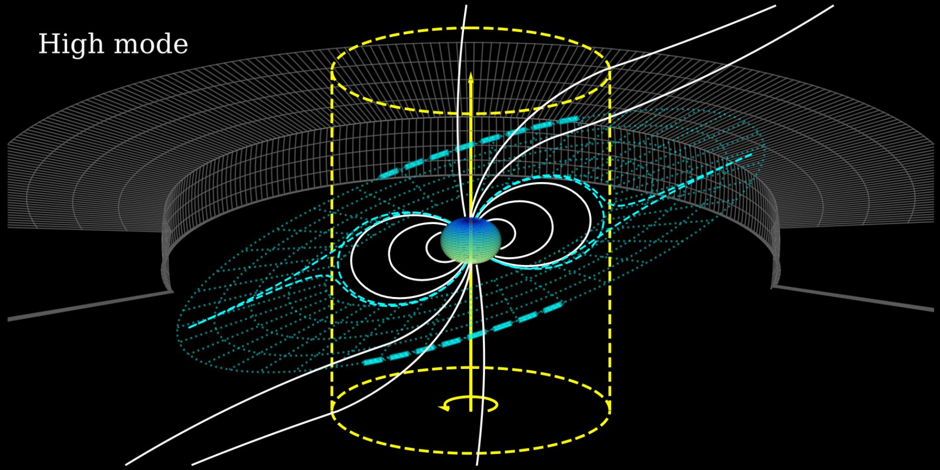

Veledina+, 2019

The proposed high mode

Accretion rate remains rather low

The system exhibits the high mode when the disk inner edge is outside Rlc

The disk occasionally penetrates the light cylinder

⬇

Transition to low mode

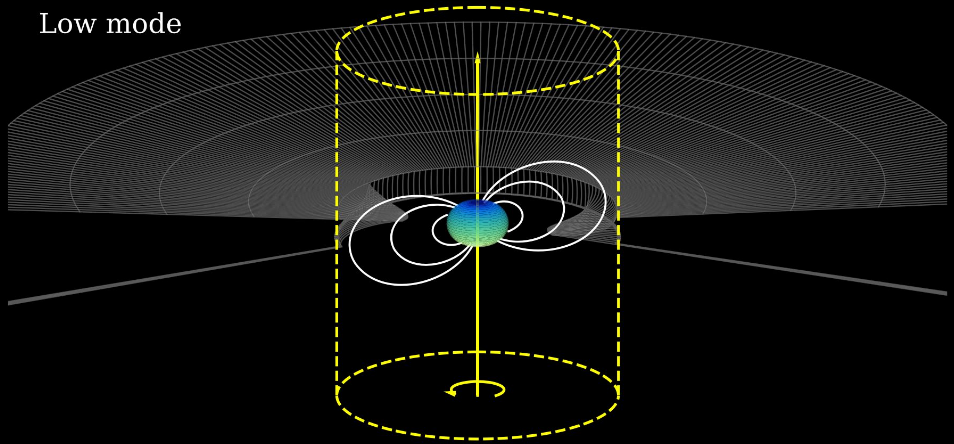

Veledina+, 2019

The proposed high mode

Strong equatorial pulsar wind bombards the inner edge of the disk, enhancing the dissipation rate and the X-ray luminosity from the system.

The wind powers has a strong fan-like peak around the current sheet that extends outside the light cylinder

A misalignment implies that the fan of the wind peak slides along the inner edge of the disk as the pulsar rotates

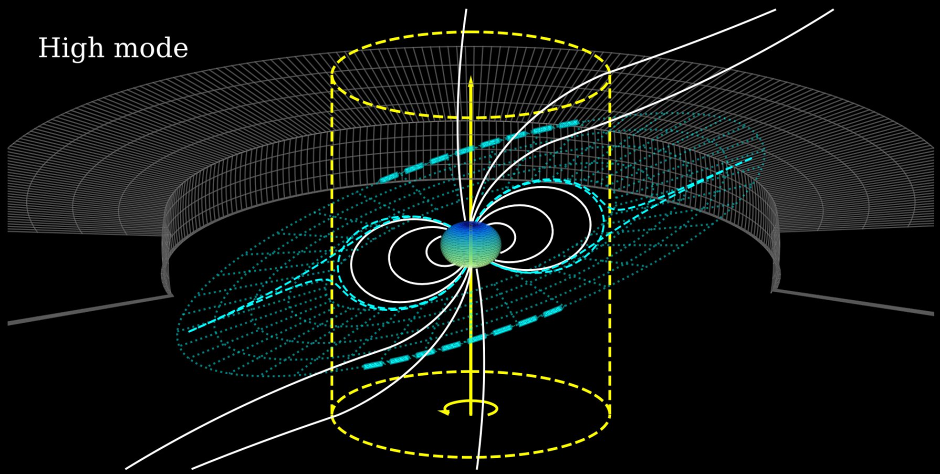

The energy dissipated in the wind–disk collision is radiated via synchrotron (and inverse Compton) mechanism.

High mode energetics

The high mode of PSR J1023+0038 in this picture is powered by the rotation energy extracted from the pulsar, carried by its wind, and eventually radiated by the disk.

The wind dissipation is expected to increase in the presence of a disk outside the light cylinder, as the disk forms an obstacle for the pulsar wind.

The pulsar wind power is known from observations during the rotation powered state, when there is no accretion

$$L_{\rm sd} \approx 4 \times 10^{46} \dot{P}_{\rm RP} P^{-3} \sim 4.4 \times 10^{34}\ \mathrm{erg\ s^{-1}}$$

Veledina+, 2019

High mode energetics

The disc intercepts only part of the wind

The power dissipated in the wind–disk collision

$$\zeta_w \equiv \frac{L_{diss}}{L_{sd}} \gtrsim \frac{H}{R}$$

disc thickness

radius of interest

sufficient to generate the high mode luminosity

depends on the misalignment angle between the magnetic dipole moment is then and the pulsar angular velocity

Veledina+, 2019

How is radiation produced?

Collision between the pulsar wind and the disk involves shocks

⬇

Deposits energy into the disk turbulence

The average energy per particle in a pulsar wind is

wind power

$$\eta = \frac{L_{\rm sd}}{\dot{N}_{\rm w} m_{\rm e} c^2}$$

rate of particle ejection in the wind

Veledina+, 2019

How is radiation produced?

This implies a huge Lorentz factor and emission from such energetic particles does not give a high radiative efficiency in the X-ray band

⬇

The observed X-ray luminosity cannot be emitted by heated wind particles

$$\eta = \frac{L_{\rm sd}}{\dot{N}_{\rm w} m_{\rm e} c^2}$$

Veledina+, 2019

How is radiation produced?

Let's consider disc particles.

The particles inflow in the equatorial plane to the disc termination radius and get ejected as a result of energy deposition by the wind

Average energy deposited by the wind per disc particle

$$\bar{E} = \frac{\zeta_{\rm w} L_{\rm sd}}{\dot{N}}$$

particle flow rate

Veledina+, 2019

How is radiation produced?

In the shock a fraction ζ_d of the total flow of disc particles is heated in the interaction

+

A significant fraction ε_e of the heat is given to electrons

Gives this Lorentz

$$\gamma_{\rm m} \sim \epsilon_{\rm e} \frac{m_{\rm p}}{m_{\rm e}} \frac{\zeta_{\rm w} L_{\rm sd}}{\zeta_{\rm d} \dot{M} c^2} \sim 10^4 \, \epsilon_{\rm e} \frac{\zeta_{\rm w}}{\zeta_{\rm d}}$$

Veledina+, 2019

How is radiation produced?

The heated plasma quickly loses its energy via synchrotron cooling

The cooling timescale with $\gamma \gg 1$ is given by

$$t_{\rm s,cool} \approx \frac{6\pi m_{\rm e} c}{\sigma_{\rm T} B^2 \gamma} \approx \frac{8 \times 10^{-5}\ {\rm s}}{\gamma_3\, B_5^2}$$

The peak frequency of synchrotron emission by particles with Lorentz factor γ is

$$\nu_{\rm s}(\gamma) \approx 0.3\, \frac{3eB}{4\pi m_{\rm e} c}\, \gamma^2 \approx 10^{17}\, \gamma_3^2\, \epsilon_B^{1/2}\ {\rm Hz}$$

Veledina+, 2019

How is radiation produced?

Most of the dissipated energy is radiated by particles with $\gamma \sim \gamma_m$ and the emission falls in the X-ray band

The heating mechanism produces a Maxwellian distribution with the thermal Lorentz factor $\gamma \sim \gamma_m$.
As the particles are fast-cooling and the Lorentz factor decreases they radiate their energies at decreasing frequencies $\nu \sim \nu_s$

obtaining a spectral distribution of

$$\frac{dL}{d\ln\nu} \sim \frac{\zeta_d \dot{M} c^2}{\epsilon_B^{1/4}} \nu_{17}^{1/2}$$

Consistent with the observed X-ray luminosity

Veledina+, 2019

How is radiation produced?

The predicted fast-cooling photon index is $\Gamma = 1.5$ → But the observed is $\Gamma \approx 1.7$

NOT a simple synchrotron model

In addition to the synchrotron cooling, the particles are cooled by the inverse Compton (IC) process.

the electron losses to IC radiation are expected to be smaller than the synchrotron losses, at least at the inner edge of the accretion disk, where the magnetic field is strongest.

Veledina+, 2019